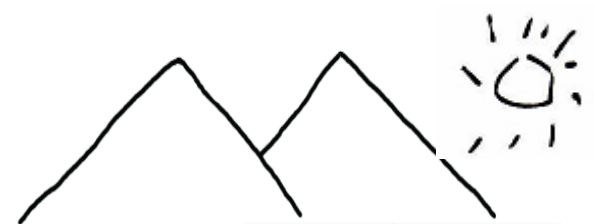


# ON

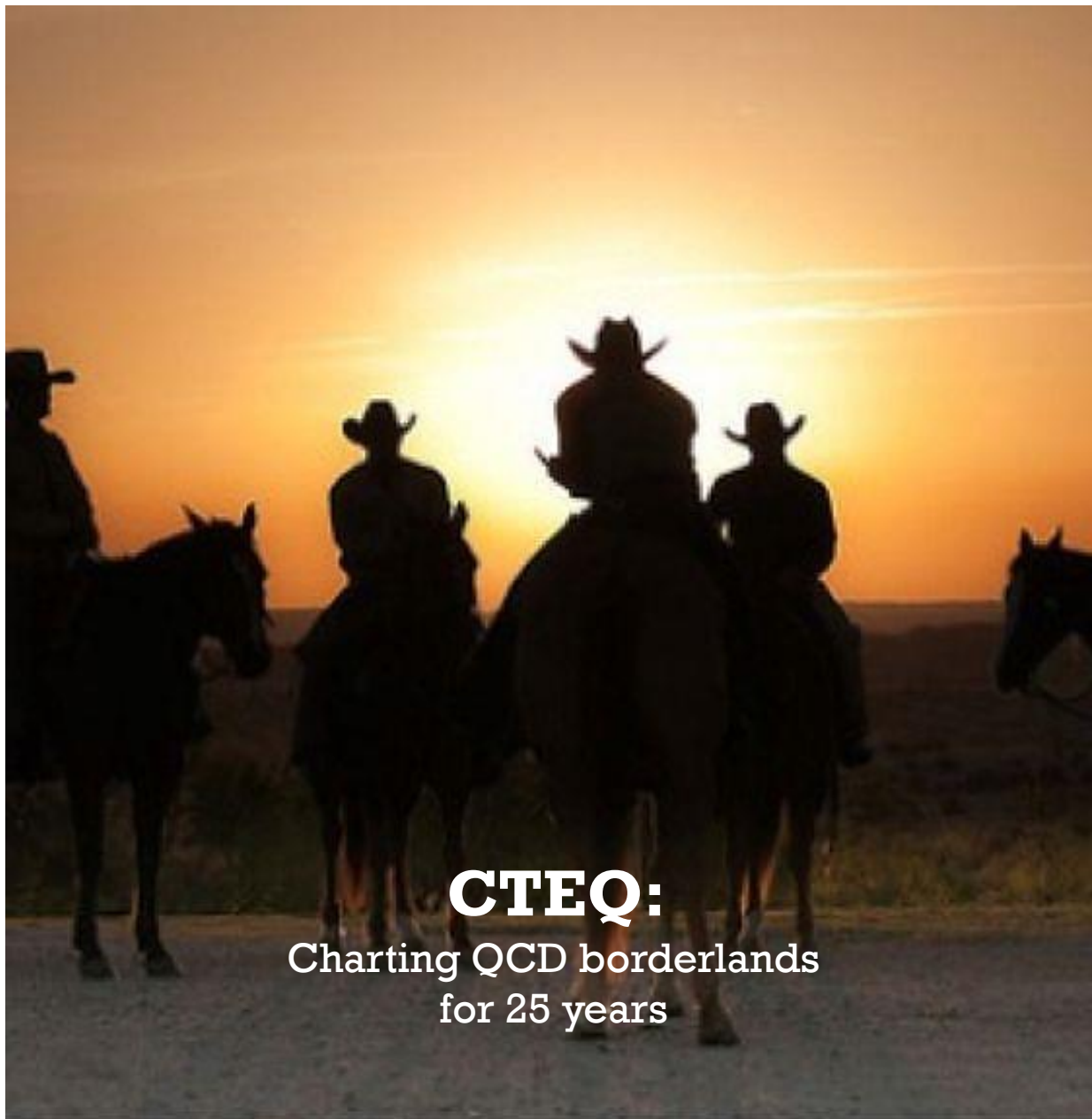
# AT THE PDF FRONTIER:

# CTEQ (TUNG ET AL.)

- Post-CT14 developments, CT14 photon PDFs
- Bridging Hessian and Monte-Carlo formalisms
  - Dependence on heavy-flavor schemes
  - Recommendations on PDF usage



**PAVEL  
NADOLSKY  
(SMU)**



**CTEQ:**  
Charting QCD borderlands  
for 25 years

**CTEQ-TEA (CT)**

Argonne: J. Gao

U. Manchester: M. Guzzi

Michigan State U.:

J. Huston, J. Pumplin,  
C. Schmidt, D. Stump,  
C. -P. Yuan

Southern Methodist U.:

T.-J. Hou, P.N. , B. Wang,  
K. Xie

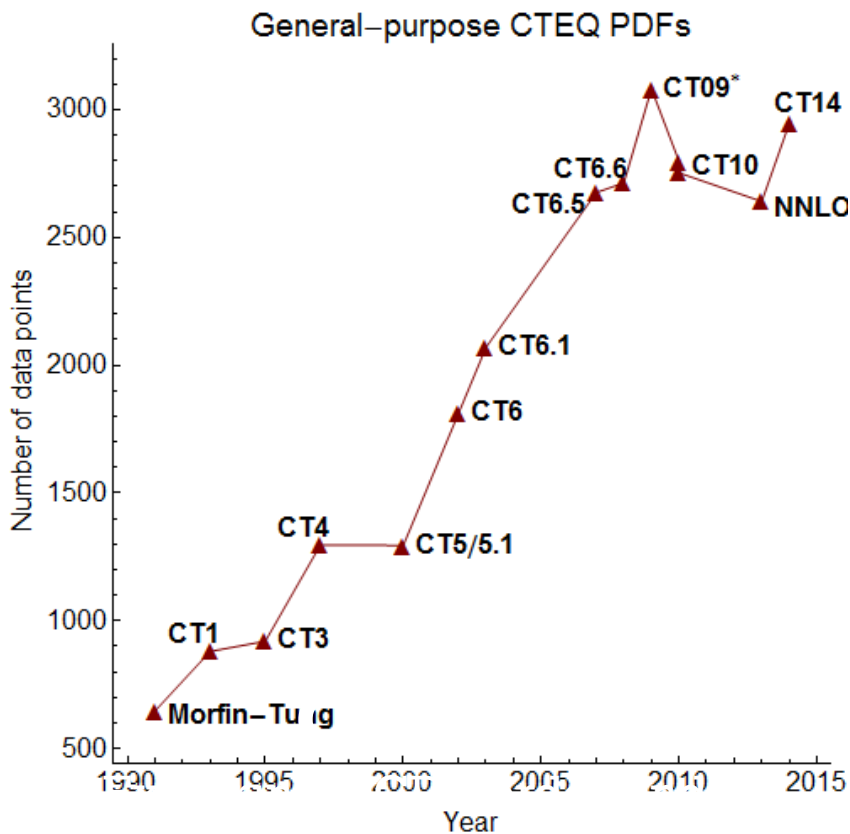
Xinjiang: S. Dulat

**+CTEQ-JLAB (CJ)**

# COORDINATED THEORETICAL EXPERIMENTAL STUDY OF QCD

**Global analysis** (term promoted by J. Morfin & W.-K. Tung in 1990):

constrains PDFs or other nonperturbative functions with data from diverse hadronic experiments



**Morfin-Tung:** DIS, low-Q Drell-Yan process

**CT1:** DIS, DY, direct  $\gamma$

**CT3:** low-x DIS, W charge asymmetry

**CT4:** - direct  $\gamma$ ; + CDF high- $p_T$  jets

**CT5/5.1:** + $\sigma_{pp}/\sigma_{pd}$  in DY process; D0 jets

**CT6:** Error PDFs; correlated syst. errors

**CT6.1:** Tevatron Run-1b jets

**CT6.5:** GM-VFN scheme; free  $s(x)$

**CT6.6:** PDF correlations

**CT09\*:** +Tevatron Run-2 jets

**CT10:** +NNLO, combined HERA, Run-2 W asymmetry

**CT14:** +LHC Run-1 W, Z, jet production

# SCOURING THE HORIZON IN 2016

## Projected Experimental Uncertainties

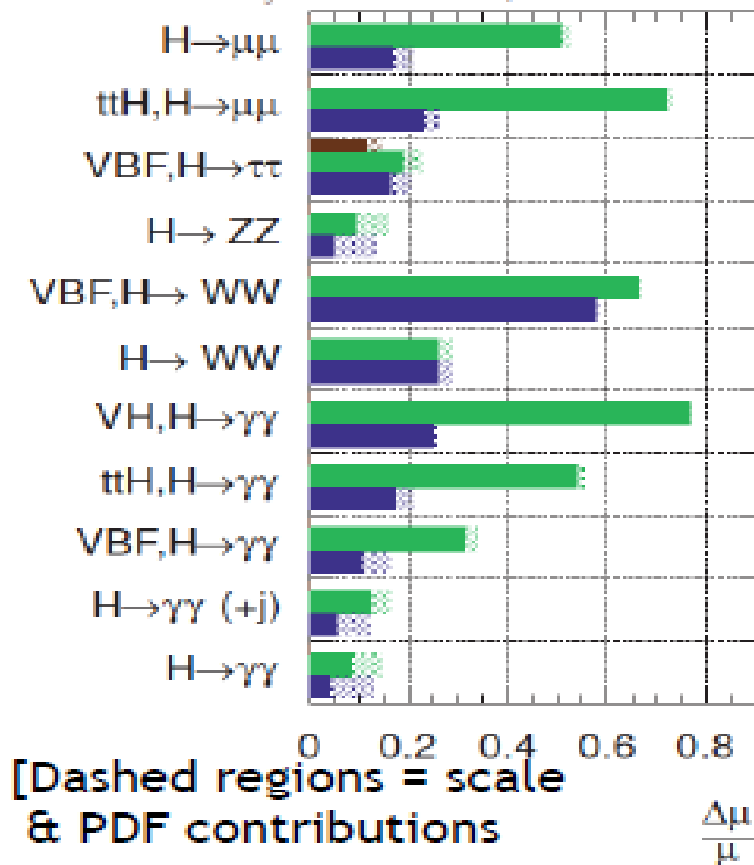
### High-luminosity LHC

- New (N)NNLO calculations likely to be completed
- Measurements of Higgs cross sections/couplings become limited by PDFs in the HL-LHC era
- Searches for non-resonant production in TeV mass range will demand accurate predictions for **sea** PDFs at  $x > 0.1$
- The target is to obtain PDFs that “achieve 1% accuracy for LHC predictions” within about a decade

ATLAS Simulation

$\sqrt{s} = 14$  TeV:  $\int Ldt=300 \text{ fb}^{-1}$  ;  $\int Ldt=3000 \text{ fb}^{-1}$

$\int Ldt=300 \text{ fb}^{-1}$  extrapolated from 7+8 TeV



# TOWARD PROTON PDFS AT 1% ACCURACY

## Theory:

1. Development of efficient techniques to estimate PDF dependence at (N)NNLO
  - a) Interfaces for fast (N)NLO computations (*Applgrid, FastNLO, aMCFast*)
  - b) Combination at the PDF level (*META, CMC*), *reduced PDFs for classes of processes*
2. Inclusion of subleading effects (NLO EM corrections, photon PDFs, off-shell resonant production...) and theoretical uncertainties (scale dependence, heavy-quark schemes, ...)
3. Special-purpose PDFs: for resummations, parton showering programs, with intrinsic charm, ...
4. Advanced statistical methods (MC, reweighting...)

# TOWARD PROTON PDFS AT 1% ACCURACY

## Experiment:

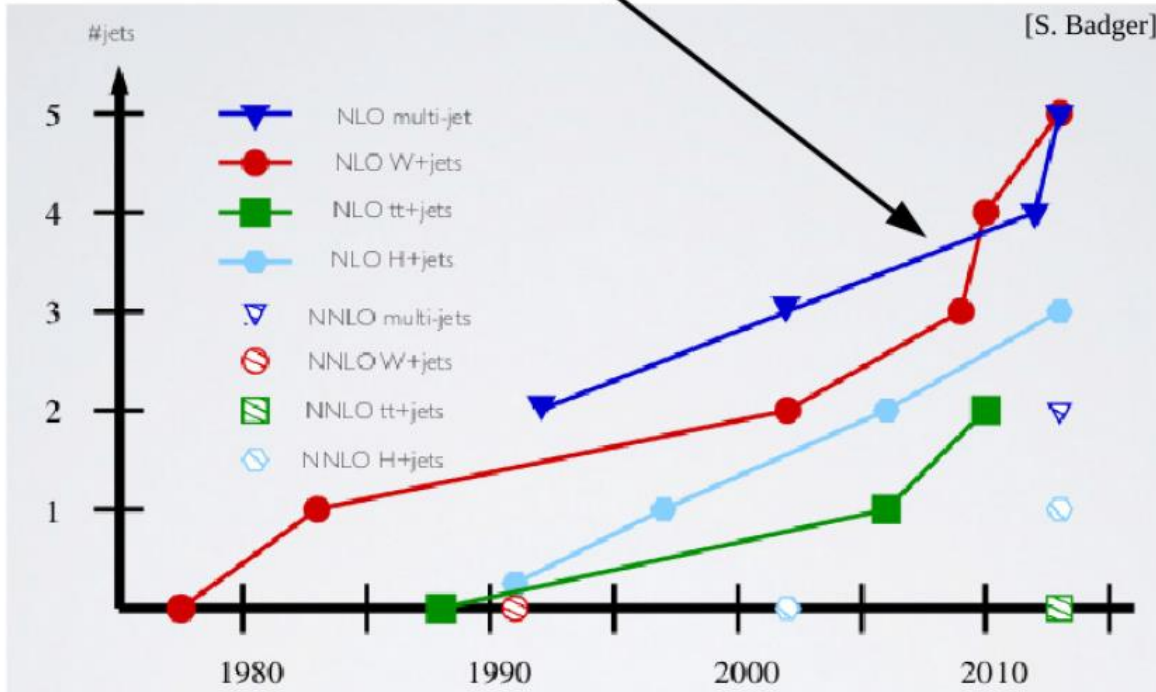
1. Finding new, highly sensitive measurements for constraining PDFs
  - a) Less inclusive, yet clean, processes (*e.g.*  $Z p_T$  at NNLO...)
  - b) Better constraints at  $x > 0.3$
  - c) Reliable flavor separation
2. Cross calibration of systematic uncertainties between the measurements
3. Smaller bin sizes, with some loss in statistics  $\Rightarrow$  better resolution on PDF  $x$  dependence

## Usage

1. Recommendations for efficient use of PDFs in practical applications
2. Compression of relevant information available in multiple available PDF ensembles
3. Combination of PDFs at the level of parametrizations; PDF4LHC15 combined PDFs from global fits

# Perturbative QCD loop revolution

The NLO Revolution



# of jets	# 1-loop Feynman diagram
1	11
2	110
3	1,253
4	16,648
5	256,265

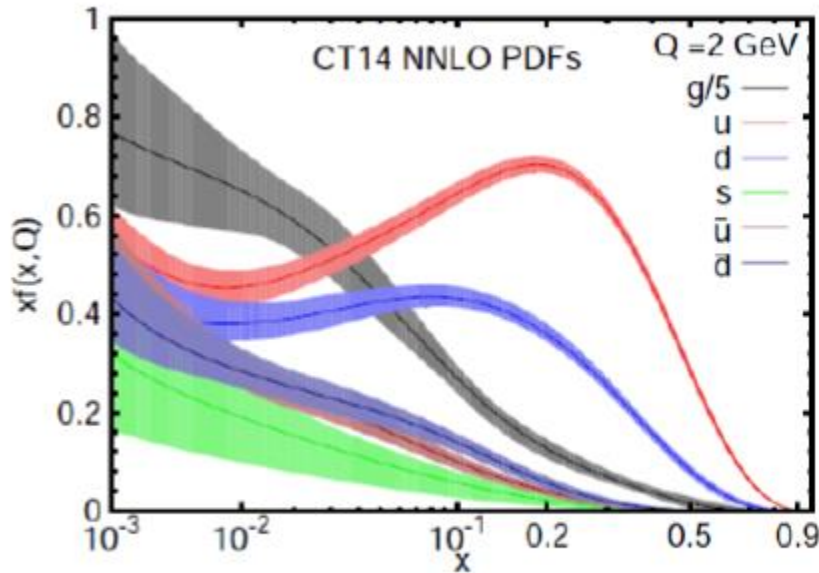
[L.Dixon]

Since 2005, generalized unitarity, sector decomposition, and related methods dramatically advanced the computations of **perturbative** NLO/NNLO/N3LO hard cross sections.

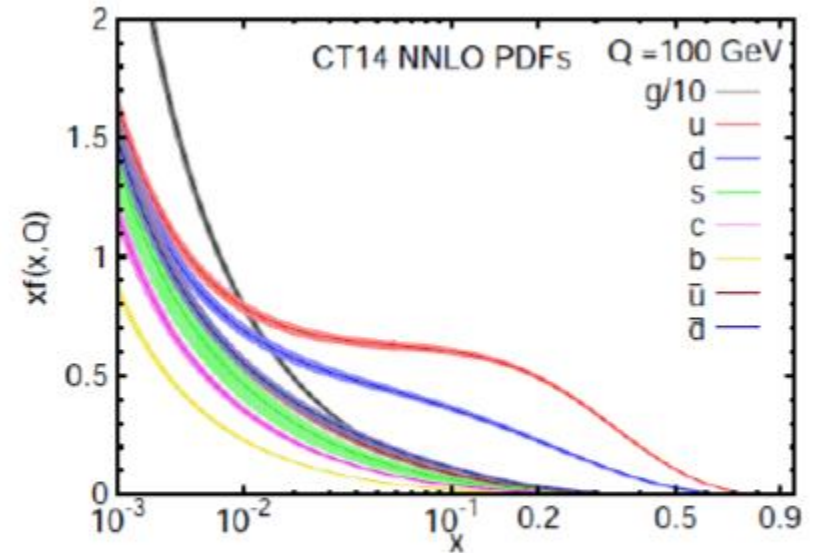
To make use of it, PDF accuracy must keep up

# General-purpose CT14 PDFs

(S. Dulat et al., arXiv:1506.07443)



$Q=2$  GeV



$Q=100$  GeV

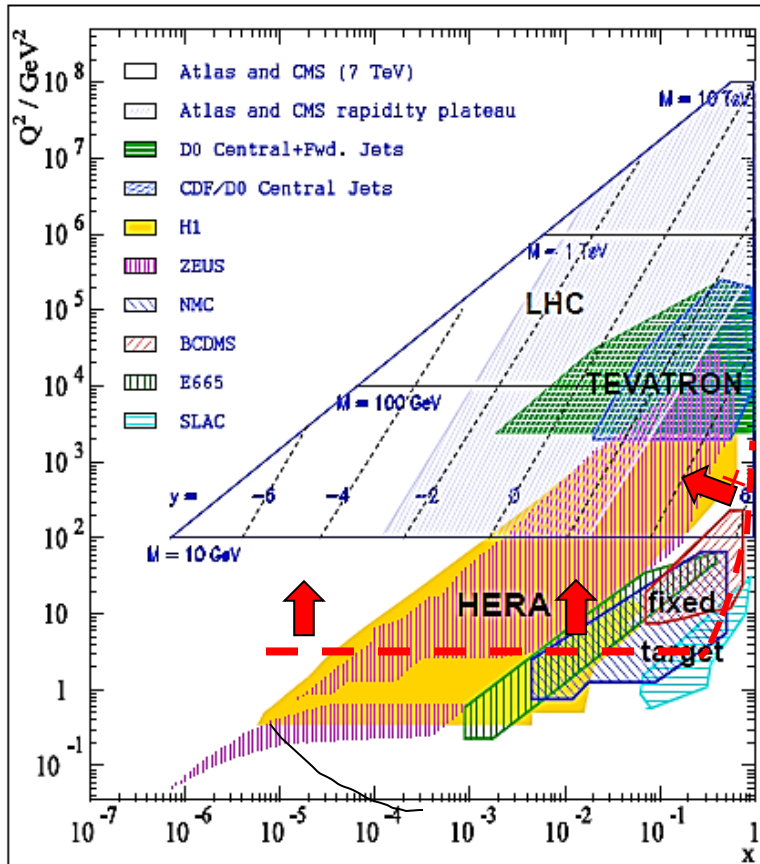
Phenomenological parametrizations of PDFs are provided with estimated uncertainties of multiple origins (**uncertainties of measurement, theoretical model, parametrization form, statistical analysis, ...**)

The shape of PDFs is optimized w.r.t. hundreds of **nuisance parameters**



# Map of experiments as a function of $x$ and $Q^2$

For nucleon PDFs, experimental measurements are selected so as to reduce dependence on theoretical input beyond the leading power in perturbative QCD



## CT14:

only DIS data with  $Q^2 > 4 \text{ GeV}^2$ ,  $W^2 > 12.25 \text{ GeV}^2$  (above the red line) are accepted to ensure stable perturbative predictions

Include LHC  $W$  asymmetry and jet production data

Still using data from DIS and DY on **nuclear targets**. CT14H2 does not use NMC DIS on deuteron, will be replaced by comparable future LHC/Tevatron measurements on **the proton**

# Experiments in the CT14 analysis

33 experiments;  $\chi^2/N_{pt} = 3252/2947 = 1.10$

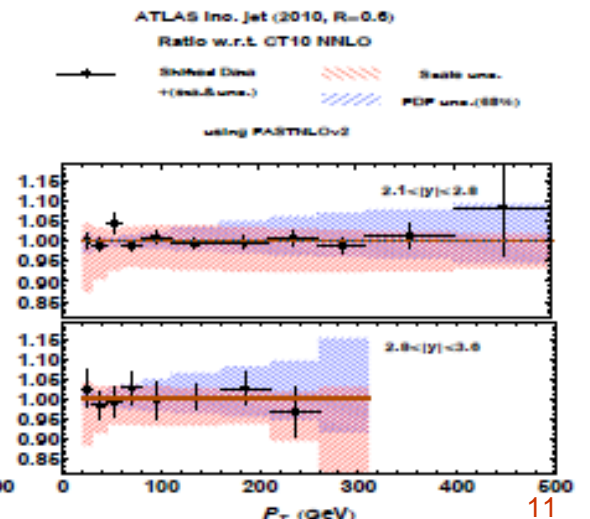
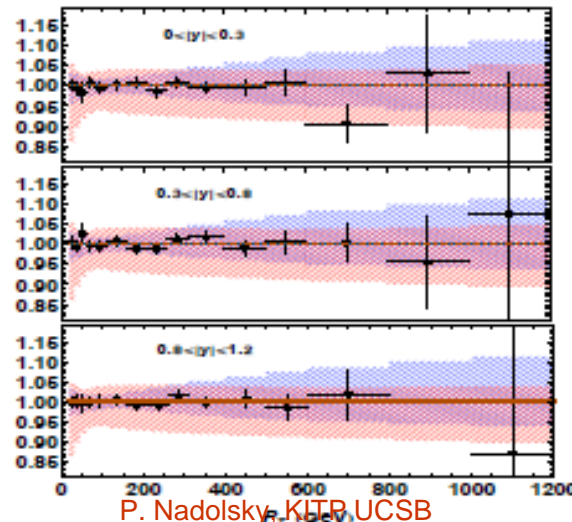
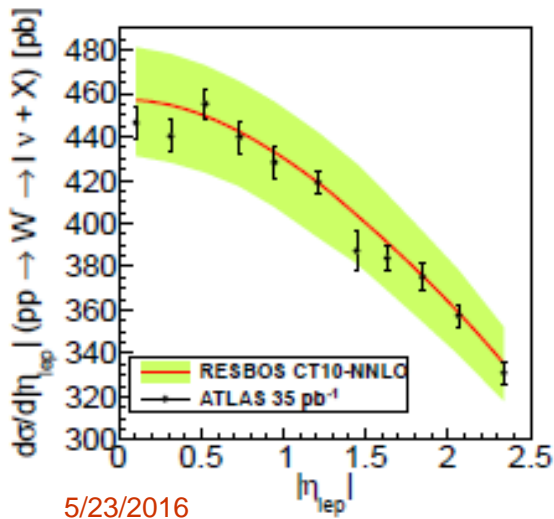
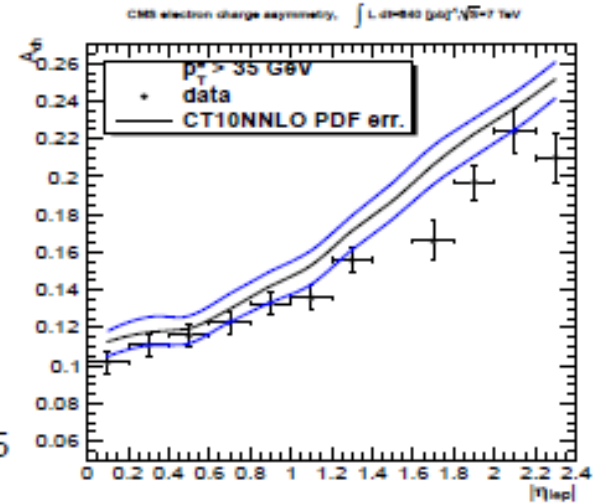
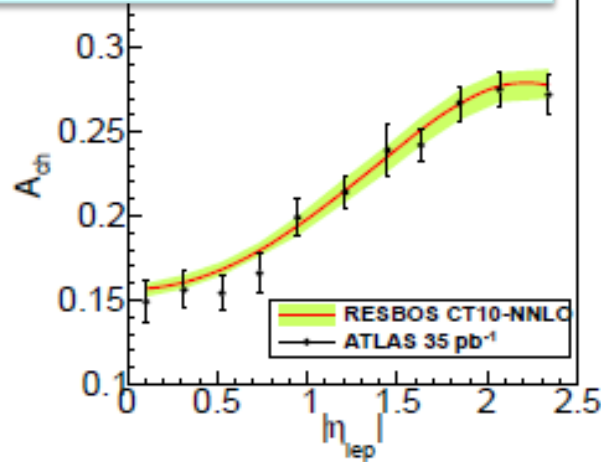
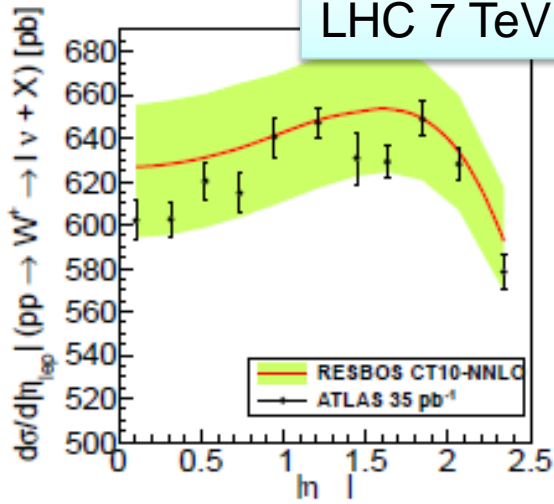
**Red arrows indicate new data sets**

Experimental data set	$N_{pt}$	$\chi_e^2/N_{pt}$
BCDMS $F_2^p$		
BCDMS $F_2^d$		
NMC $F_2^d/F_2^p$	[14]	1.08
NMC $\sigma_{red}^p$	[14]	1.85
CDHSW $F_2^p$	[15]	0.85
CDHSW $F_3^p$	[15]	0.83
CCFR $F_2^p$	[16]	1.02
CCFR $xF_3^p$	[17]	0.36
NuTeV $\nu\mu\mu$ SIDIS	[18]	0.62
NuTeV $\bar{\nu}\mu\mu$ SIDIS	[18]	1.18
CCFR $\nu\mu\mu$ SIDIS	[19]	0.72
CCFR $\bar{\nu}\mu\mu$ SIDIS	[19]	0.53
H1 $\sigma_r^b$	[20]	0.68
HERA charm production	[21]	1.26
HERA1 Combined NC and CC DIS	[22]	1.02
H1 $F_L$	[23]	1.92

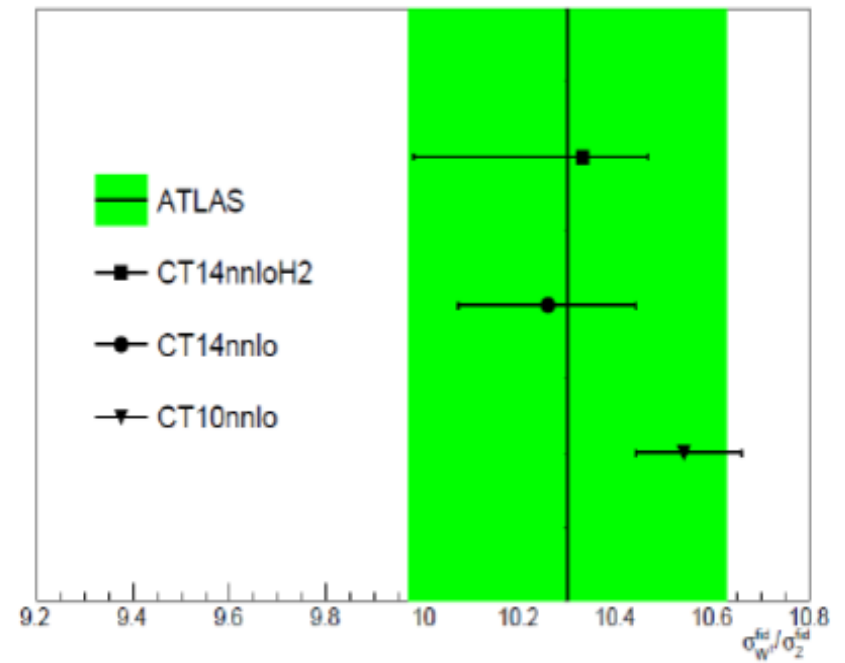
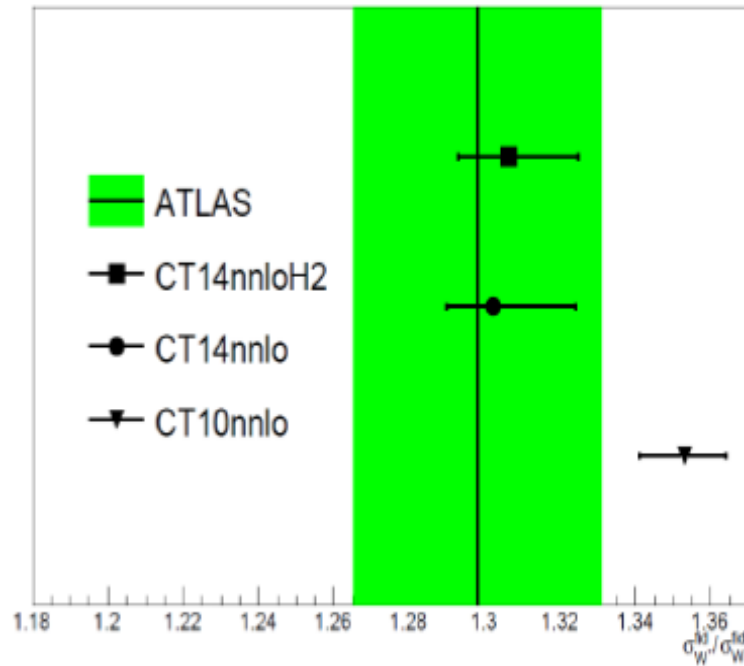
Experimental data set	$N_{pt}$	$\chi_e^2/N_{pt}$
E866 Drell-Yan	[24]	119 0.98
E866 Drell-Yan	[25]	15 0.87
E866 Drell-Yan	[25]	184 1.37
CDF Run-1 electron $A_{ch}$	[26]	11 0.81
CDF Run-2 electron $A_{ch}$	[27]	11 1.24
D0 Run-2 muon $A_{ch}$	[29]	9 0.92
LHCb 7 TeV 35 pb <sup>-1</sup> $W/Z$ $d\sigma/dy_\ell$	[31]	14 0.7
LHCb 7 TeV 35 pb <sup>-1</sup> $A_{ch}$ , $p_{T\ell} > 20$ GeV	[31]	5 1.19
D0 Run 2 $Z$ rapidity	[32]	28 0.59
CDF Run 2 $Z$ rapidity	[33]	29 1.64
CMS 7 TeV 4.7 fb <sup>-1</sup> , muon $A_{ch}$	[34]	11 0.8
CMS 7 TeV 840 pb <sup>-1</sup> , electron $A_{ch}$	[35]	11 0.87
ATLAS 7 TeV 35 pb <sup>-1</sup> $W/Z$ cross sections and $A_{ch}$	[36]	41 1.11
D0 Run-2 electron $A_{ch}$ (9.7 fb <sup>-1</sup> )	[37]	13 1.79
CDF Run-2 inclusive jet production	[40]	72 1.45
D0 Run-2 inclusive jet production	[41]	110 1.09
ATLAS 7 TeV 35 pb <sup>-1</sup> incl. jet production	[42]	90 0.55
CMS 7 TeV 5 fb <sup>-1</sup> incl. jet production	[43]	133 1.33

# CT10 NNLO PDFs do not include LHC data, but **predict** LHC Run-1 observables well

LHC 7 TeV data vs CT10 NNLO PDFs



# The ratios of $W^+$ to $W^-$ and $(W^++W^-)$ to $Z$ cross sections CT14HERA2 vs. CT14

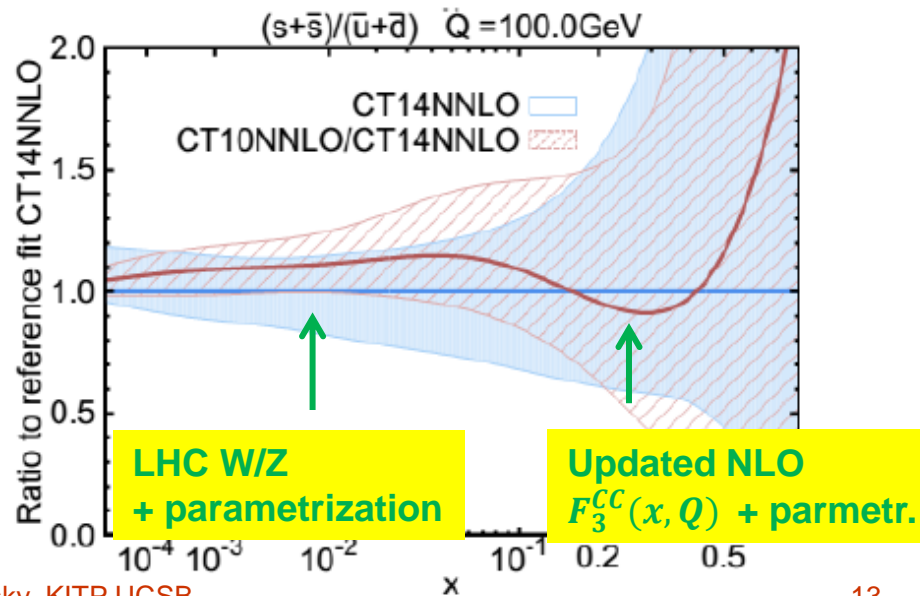
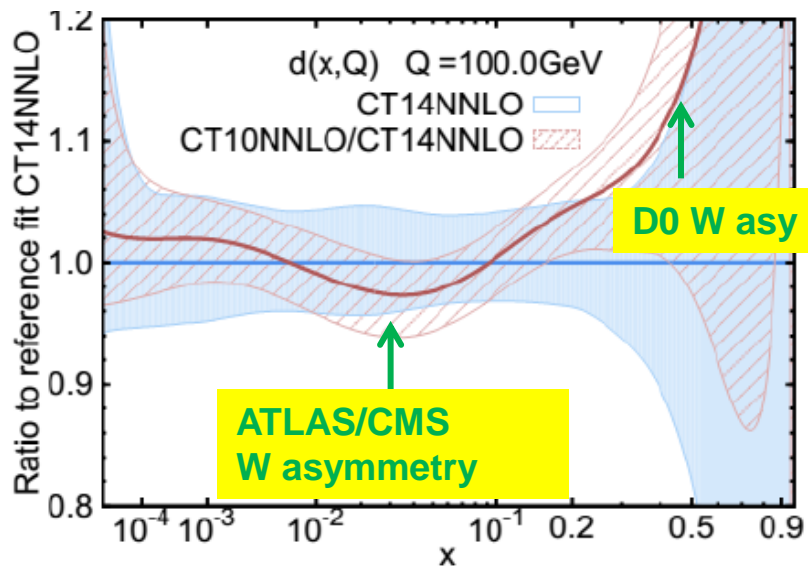
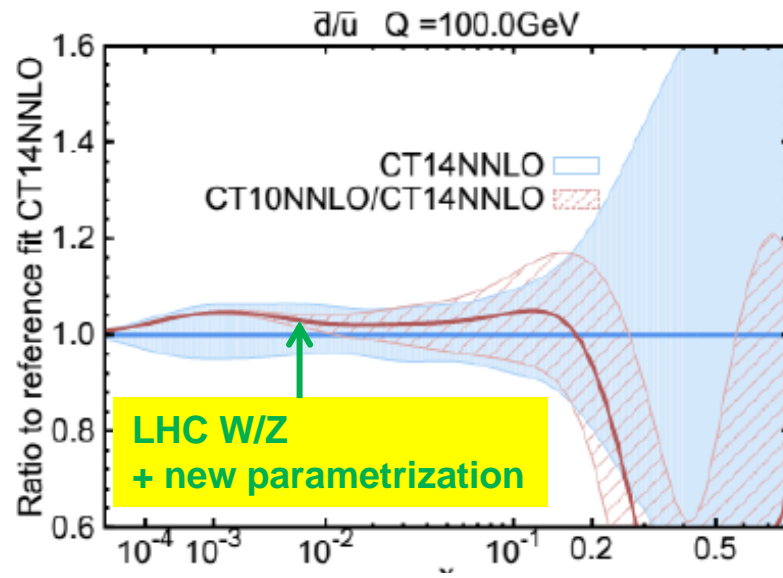
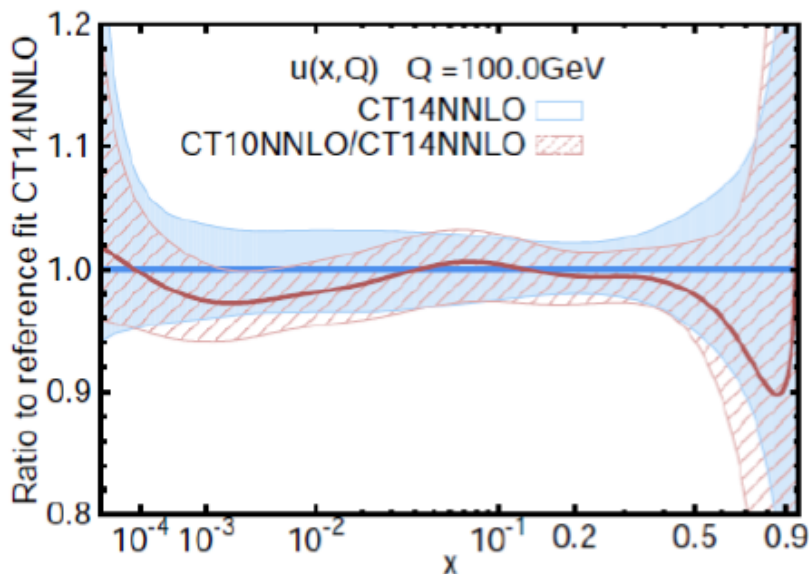


$$p_T^l > 25 \text{ GeV}, \quad |\eta_l| < 2.5, \quad 66 < m_{ll} < 116 \text{ GeV}$$

$$p_T^l > 25 \text{ GeV}, \quad p_T^\nu > 25 \text{ GeV}, \quad |\eta_l| < 2.5, \quad m_T > 50 \text{ GeV}$$

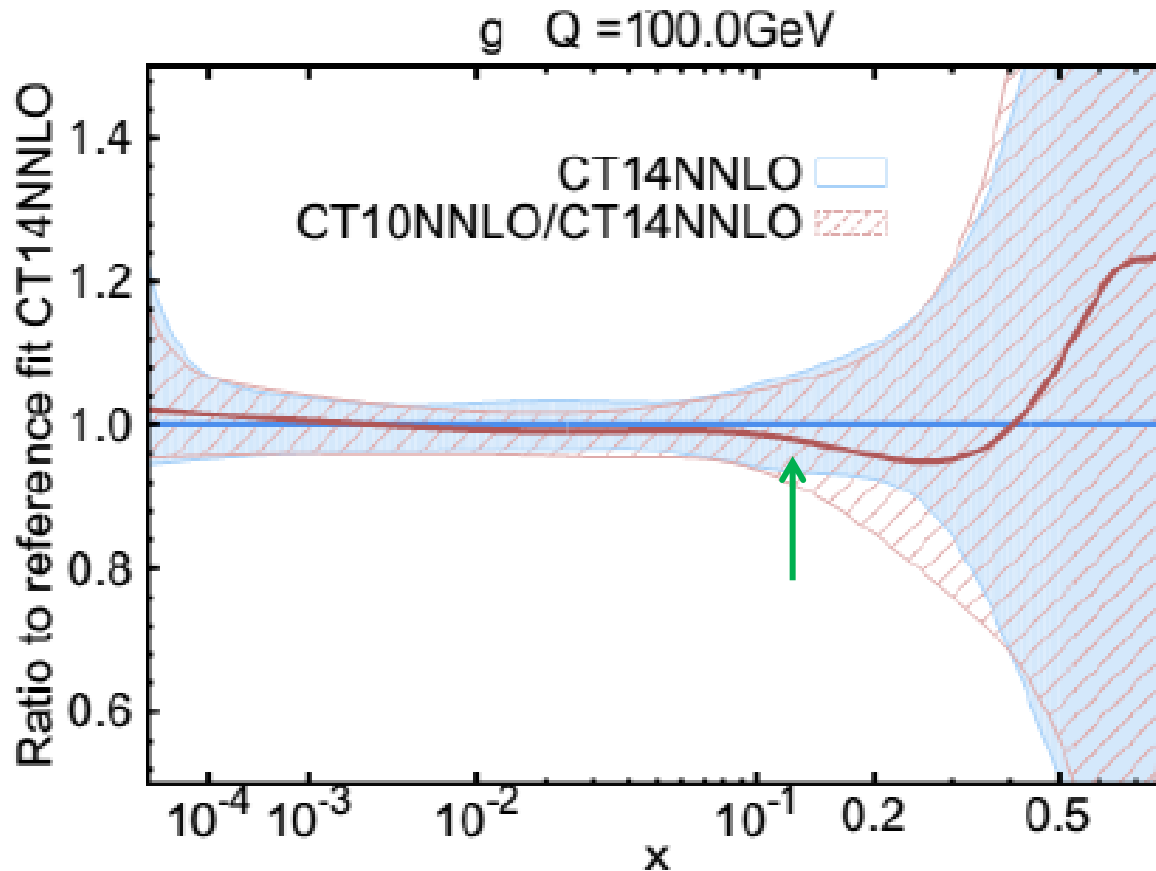
A rare exception

# Compare CT14 and CT10 quark PDFs

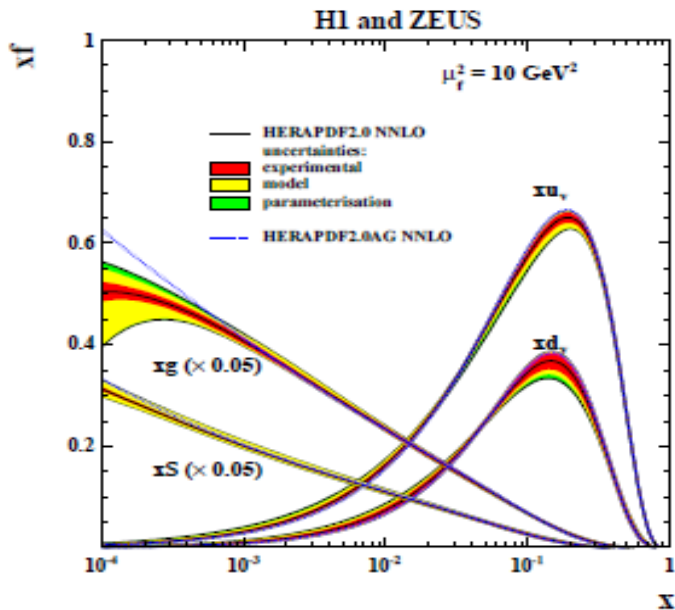


# CT14 vs. CT10: the gluon PDF

$g(x, Q)$  is slightly higher in CT14 at  $x \sim 0.05$  because of several effects.



CT14 Higgs cross sections increase compared to CT10 by about 1-2%

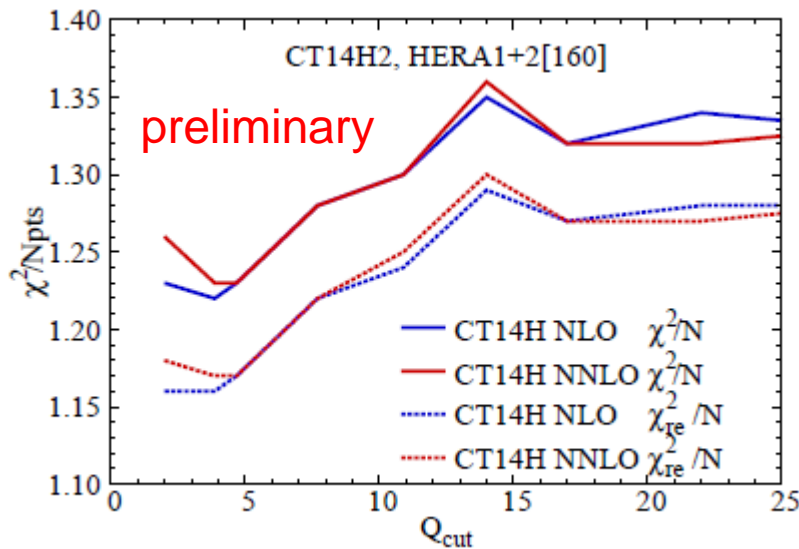


The combined HERA1+2 data are included in HERA2.0, **CT14HERA2**, MMHT, and NNPDF3.1 analyses

$\chi^2/d.o.f. \sim 1.2$  for HERA1+2 tends to be elevated across all analyses, compared to  $\chi^2/d.o.f. < 1.1$  for combined HERA1 data

⇒ This tension may arise from several sources

- Higher-twist corrections to  $F_L(x, Q)$
- Small- $x$ /saturation
- Experimental systematics (?)

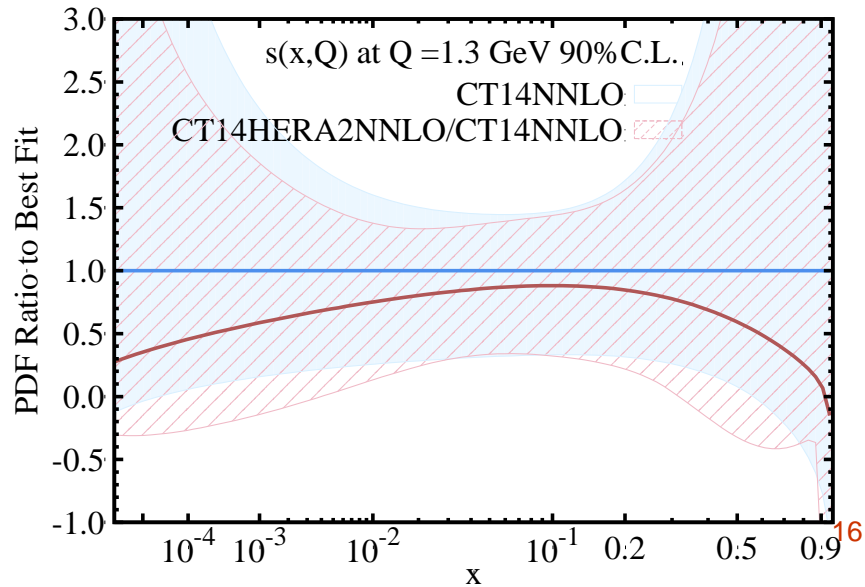
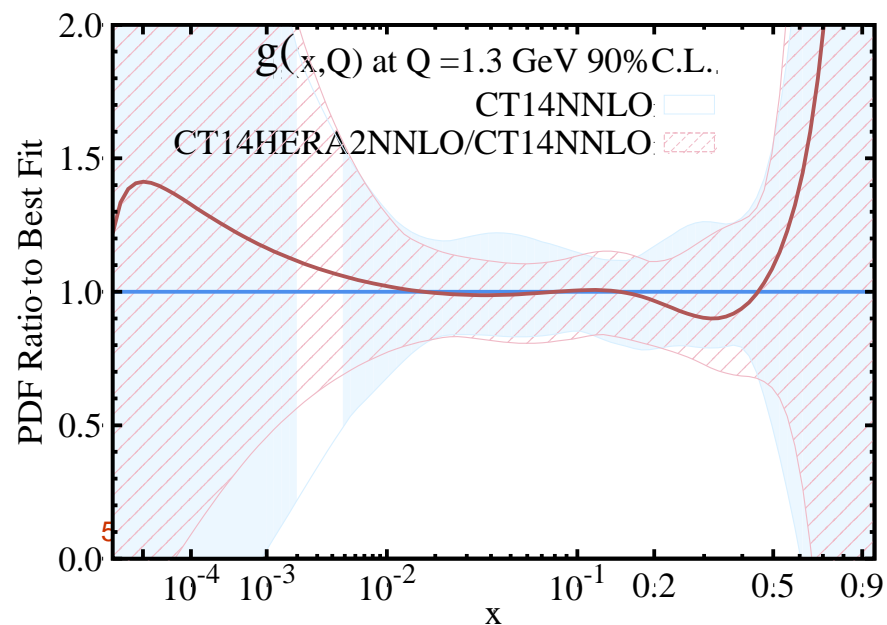
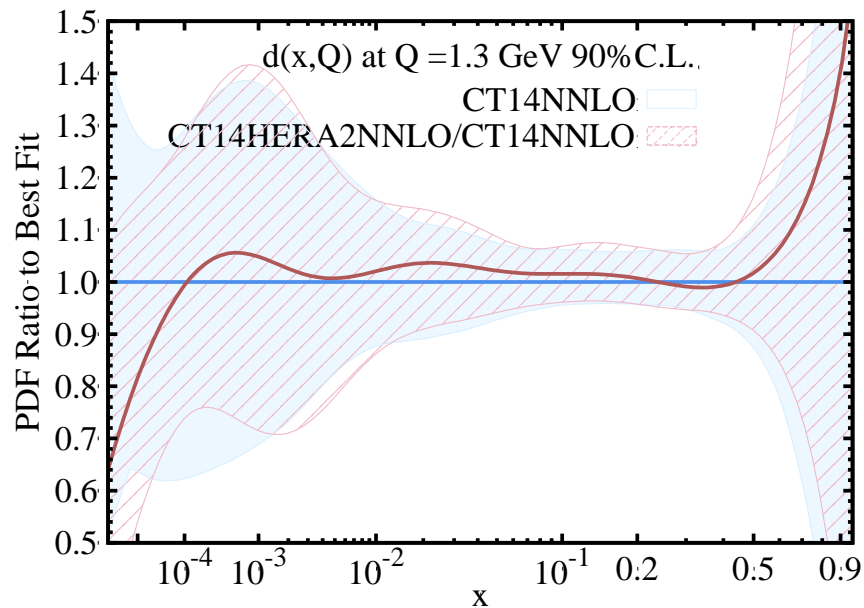
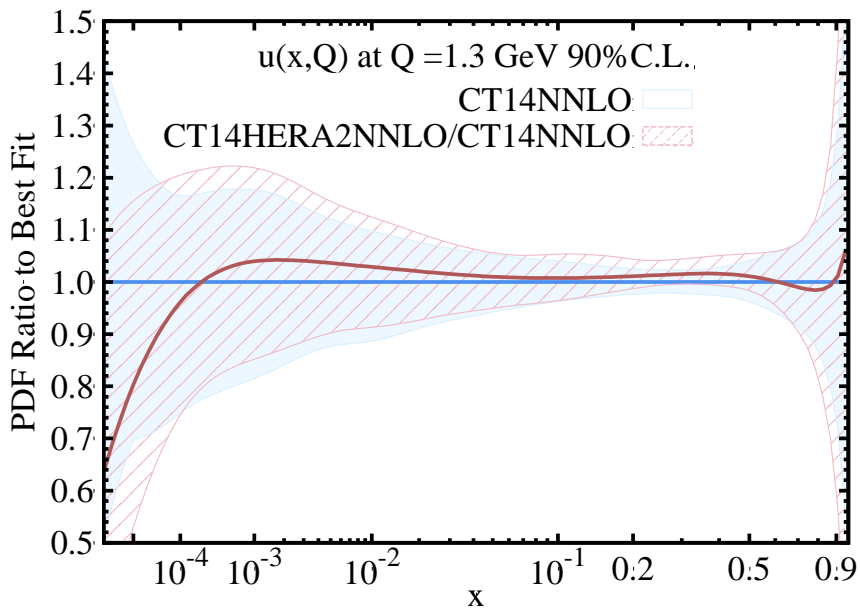


**The impact on global PDFs is mild, changes in PDFs do not exceed uncertainties**

$\chi^2/N_{pts}$  with (top) and without (bottom)

penalty for syst. shifts

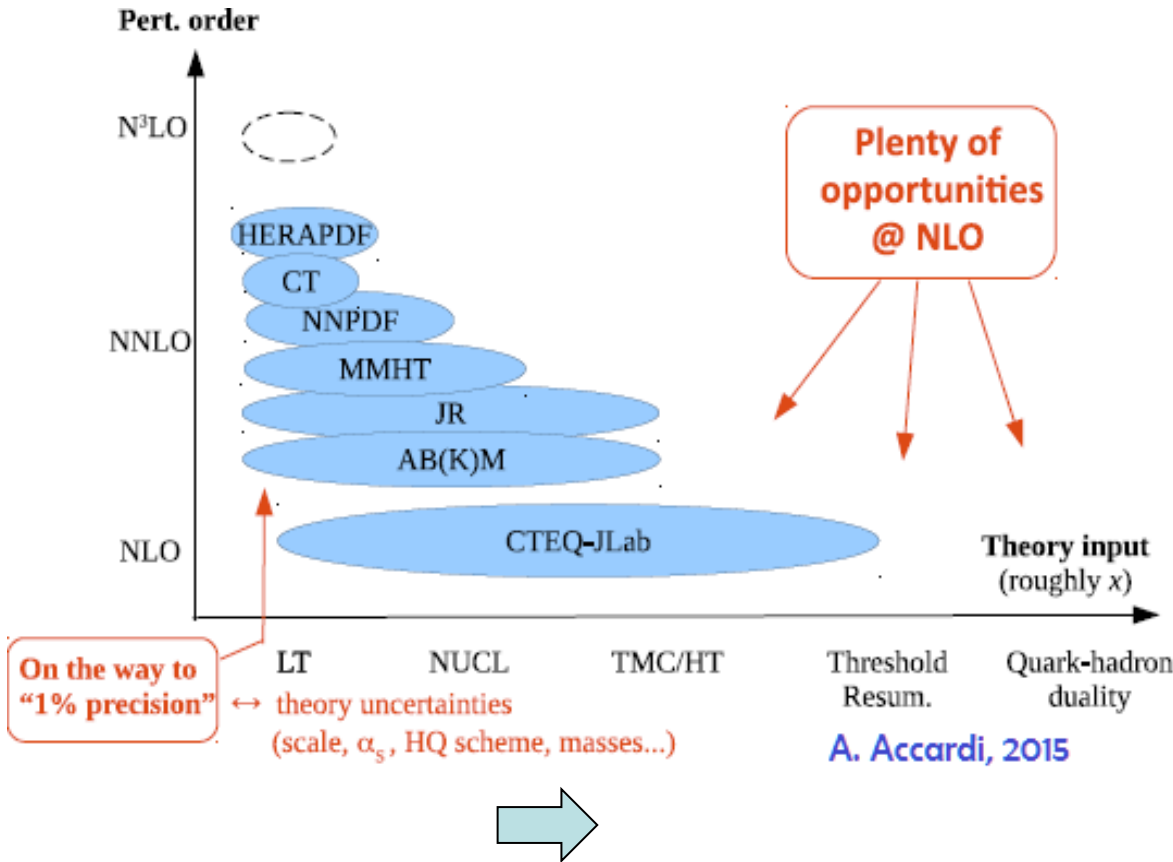
# CT14HERA2 vs. CT14 at NNLO





# 2. Specialized PDFs at NLO and NNLO

Are obtained under special assumptions or for special goals. May or may not be suitable for general physics



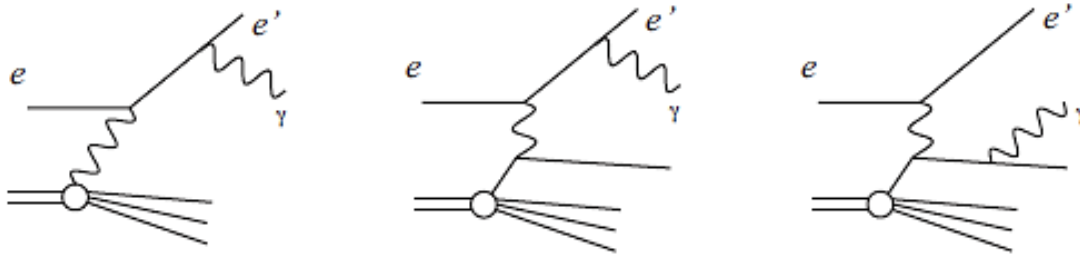
1. **CJ15:** NLO PDFs with large- $x$ /low  $Q$  DIS data
2. **Most groups:** PDFs with up to 3, 4, 6 active flavors
3. **CT, NNPDF, MSTW:** QCD+QED PDFs
4. **CT, NNPDF:** PDFs with intrinsic charm
5. **NNPDF:** PDFs for threshold resummation
6. ...

# Photon PDFs

- Still in exploratory stage – limited experimental constraints, further theory developments needed (full NNLO QCD+(N)LO EM DGLAP evolution code, consistent EW corrections to all fitted cross sections)
- $u^p(x, Q) \neq d^n(x, Q)$  -- need more data to resolve difference
- **MRST QED** PDFs (hep-ph/0411040) :  $f_\gamma^p(x, Q_0)$  is constructed from  $u_v^p(x, Q_0)$ ,  $d_v^p(x, Q_0)$ ,  $P_{\gamma \leftarrow q}(x)$
- **NNPDF2.3 QED** (1308.0598): NN parametrization for  $f_\gamma^p(x, Q_0)$ , sequential QCD+QED evolution
- **CT14 QED** (1509.02905): generalized MRST  $f_\gamma^p(x, Q_0)$ , include  $ep \rightarrow e\gamma X$  ZEUS data to constrain  $f_\gamma^p(x, Q_0)$
- **CT14QEDinc** PDFs (new): photon PDFs with the elastic production component as the input condition at  $Q_0$

# CT14 QED PDFs

C. Schmidt, J. Pumplin, D. Stump, C.-P. Yuan, arXiv:1509.02905



ZEUS  $ep \rightarrow e\gamma X$  data  
( $N_{pt} = 8$ ) included to  
constrain  $f_\gamma(x, Q)$

$$|M|_{\gamma\gamma}^2$$

$$|M|_{LL}^2$$

$$|M|_{QQ}^2 + \text{interference}$$

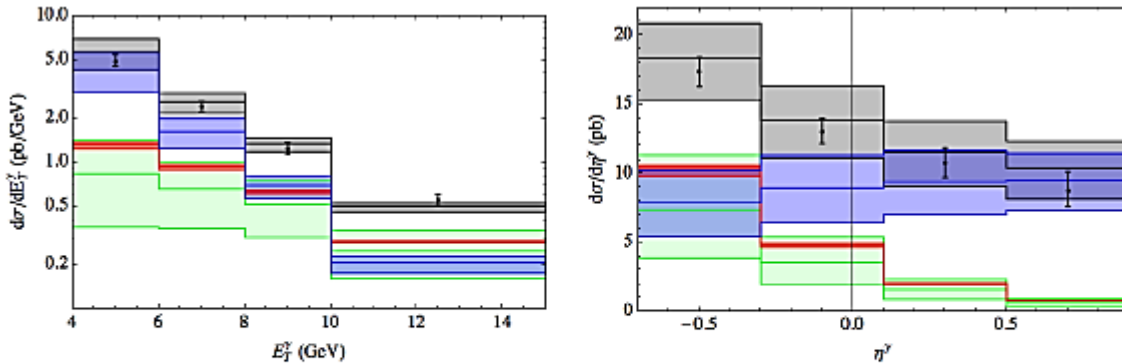


FIG. 4: Differential distributions for a zero initial photon PDF and using the smooth isolation prescription. The various bands display a variation in factorization scale between  $0.5E_{\perp\gamma} \leq \mu_F \leq 2E_{\perp\gamma}$  and correspond to the total prediction (gray), the  $QQ$  component (blue), the  $LL$  component (red), and the photon-initiated contribution only (green).

Sharp cone and smooth cone photon isolations tried; rule out the “current-mass” radiative ansatz for  $f_\gamma(x, Q_0)$  despite sizable theory uncertainties

# CT14 QED PDFs

C. Schmidt, J. Pumplin, D. Stump, C.-P. Yuan, arXiv:1509.02905

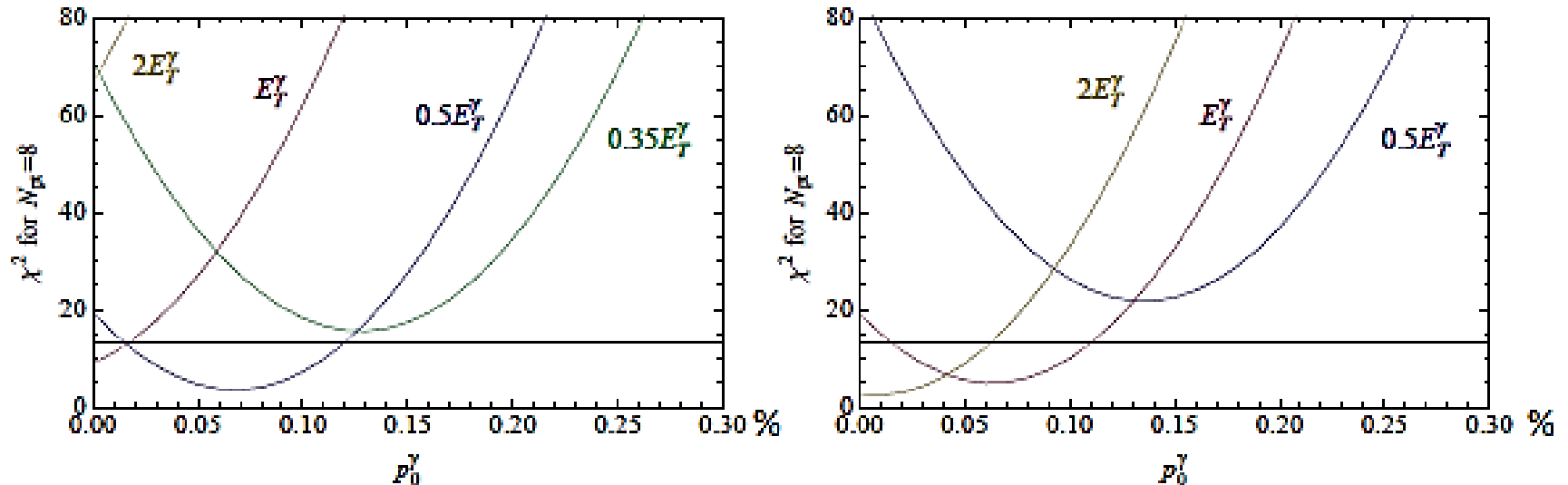
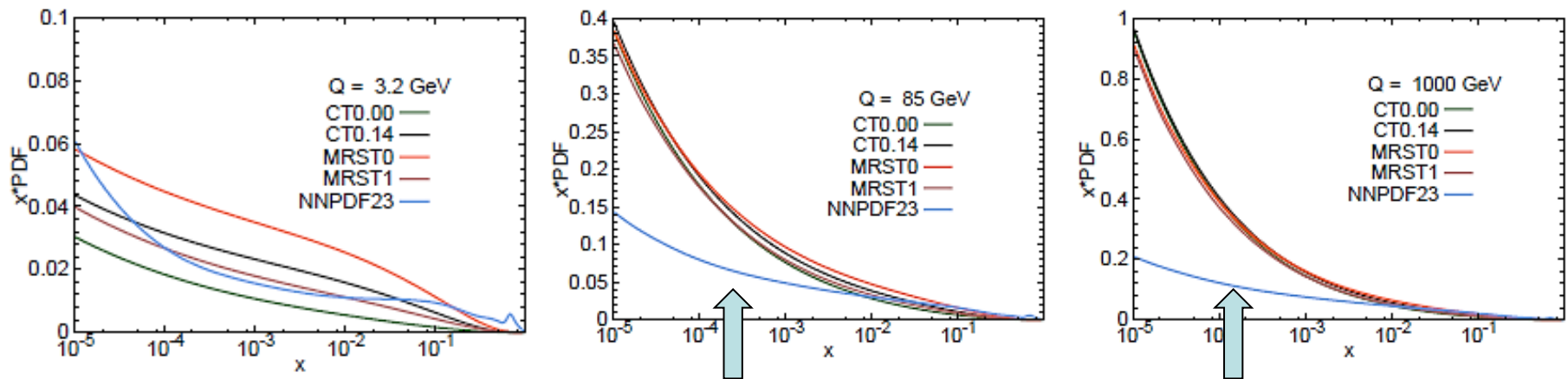


FIG. 9: Plots of  $\chi^2$  versus initial photon momentum fraction  $p_0^\gamma$  using the smooth isolation prescription (left) and the sharp isolation prescription (right) for factorization scales  $\mu_F = 2E_{\perp\gamma}$ ,  $E_{\perp\gamma}$ ,  $0.5E_{\perp\gamma}$ , and  $0.35E_{\perp\gamma}$ . The horizontal line at  $\chi^2 = 13.36$  is the 90% confidence level limit for 8 data points.

**Photon momentum fractions > 0.14% are disfavored, for the given isolation models**

# NLO photon PDFs at $Q=3.2, 85, 1000$ GeV

CT14QED with  $p_0^\gamma = 0\%$  (green), CT14QED with  $p_0^\gamma = 0.14\%$  (black), MRST2004QED0 using current quark masses (orange), MRST2004QED1 using constituent quark masses (brown), and NNPDF2.3QED with  $\alpha_s = 0.118$  and average photon (blue).



Slower DGLAP evolution of NNPD2.3 due to the factorized approximation for QCD+QED evolution operator ?

Uncertainty bands cover all central predictions



# Photon-Photon Luminosity

CTEQ

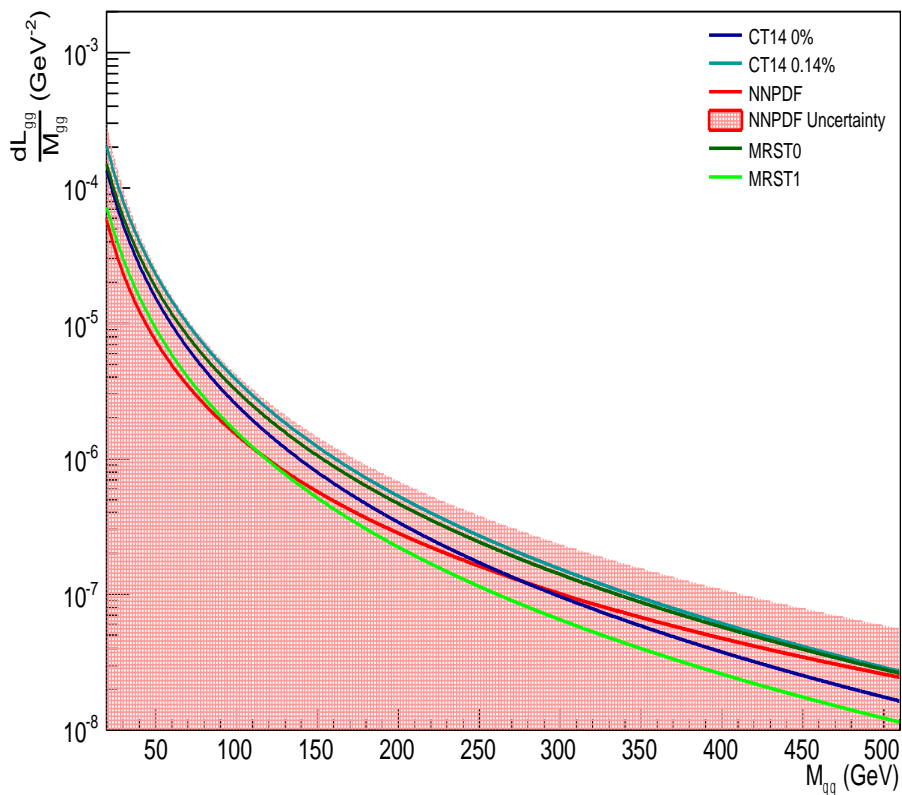


FIG. 4: Photon-photon luminosity for an invariant mass of 20 GeV to 500 GeV for 13 TeV collider energy

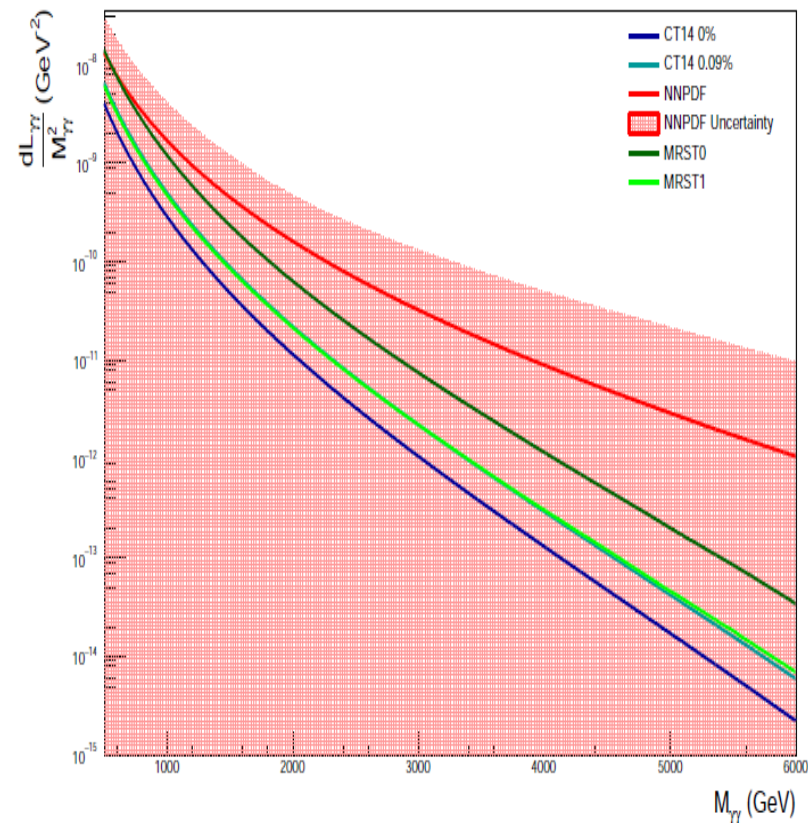


FIG. 5: Photon-photon luminosity for an invariant mass of 500 GeV to 6000 GeV for 13 TeV collider energy

- Central NNPDF photon harder at large  $x$ .



# CT14QED Photon PDFs

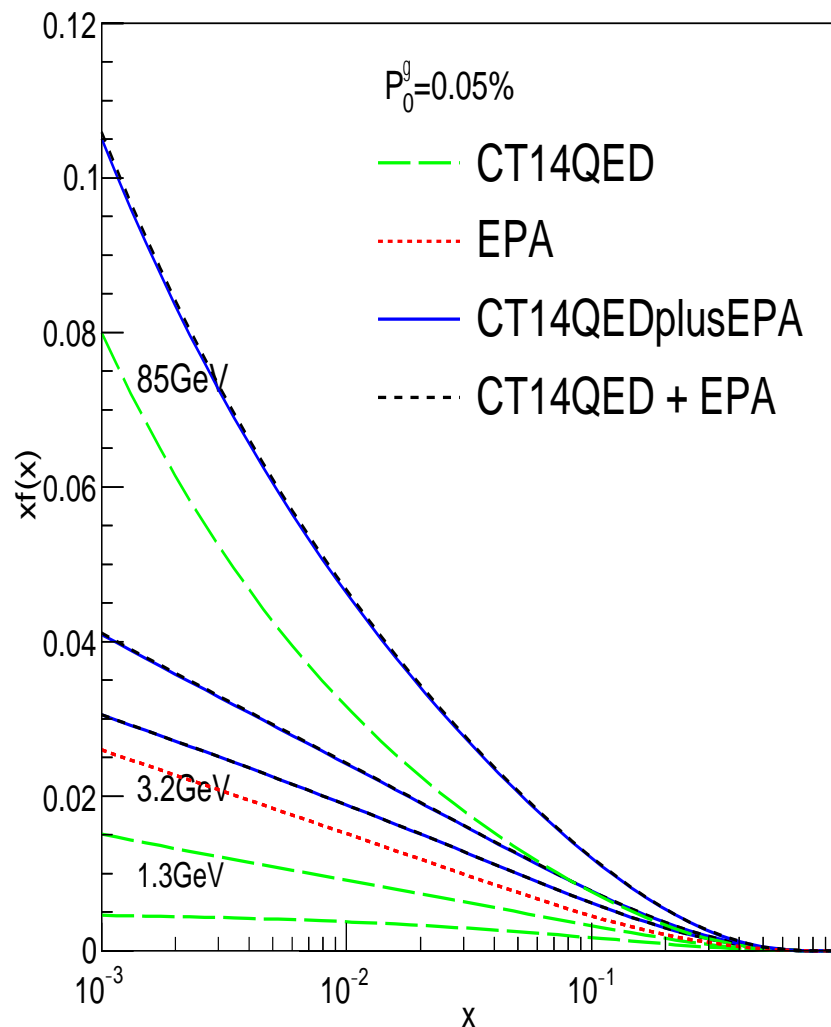
CTEQ

- Important point:

$$(f_{\text{EPA}} + f_{\text{inelastic}})(x, Q) \gg f_{\text{EPA}}(x, Q) + f_{\text{inelastic}}(x, Q)$$

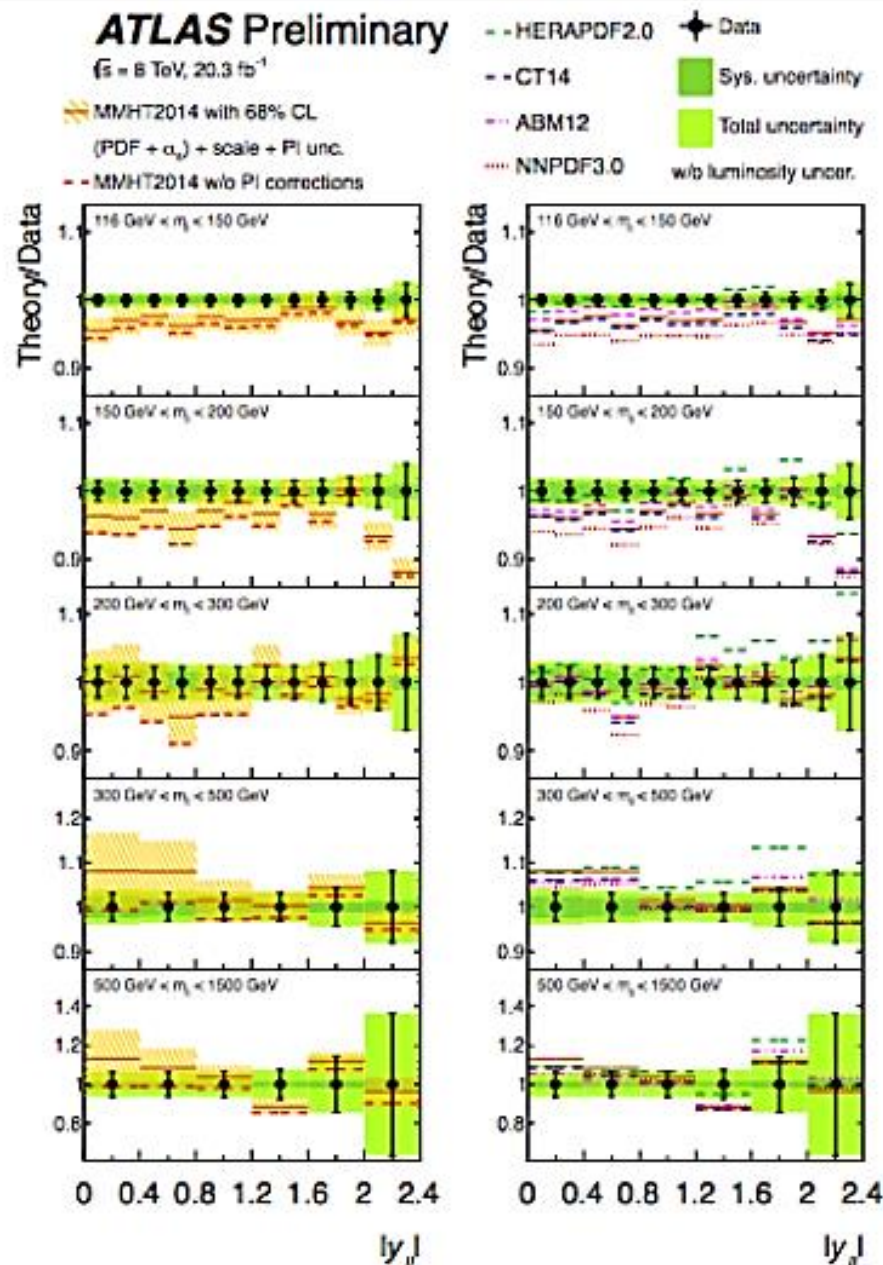
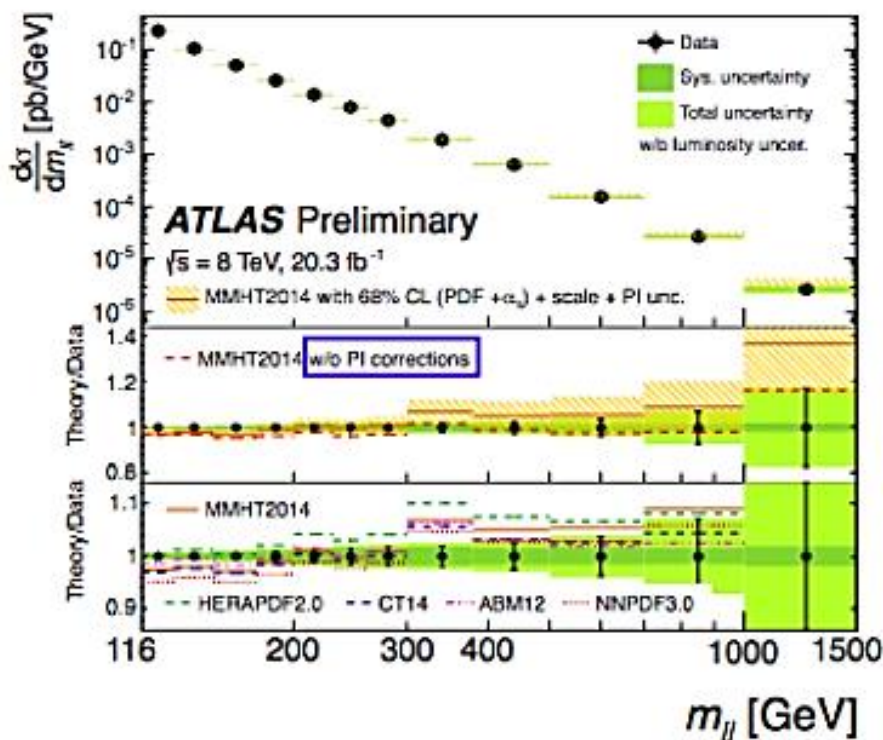
- $f_{\text{EPA}}(x, Q)$  changes little from  $Q_0$  to  $Q$  because of falloff from form factor
- Up to corrections of order  $\alpha$ , the photon PDF evolves additively:

$$f(x, Q) \approx f(x, Q_0) + \int_{Q_0^2}^{Q^2} \frac{dQ^2}{Q^2} \frac{\alpha}{2\pi} P_{\gamma q} \circ \sum e_q^2 f_q(x, Q)$$



# High mass Drell-Yan: results and comparison to theory II/II

- The measured cross-sections are compared to theoretical predictions using a selection of **recent PDFs**.
- Theory uncertainties are larger than measurement uncertainties  $\Rightarrow$  potential for PDF constraints.
- Photon induced contribution reaches 15%.

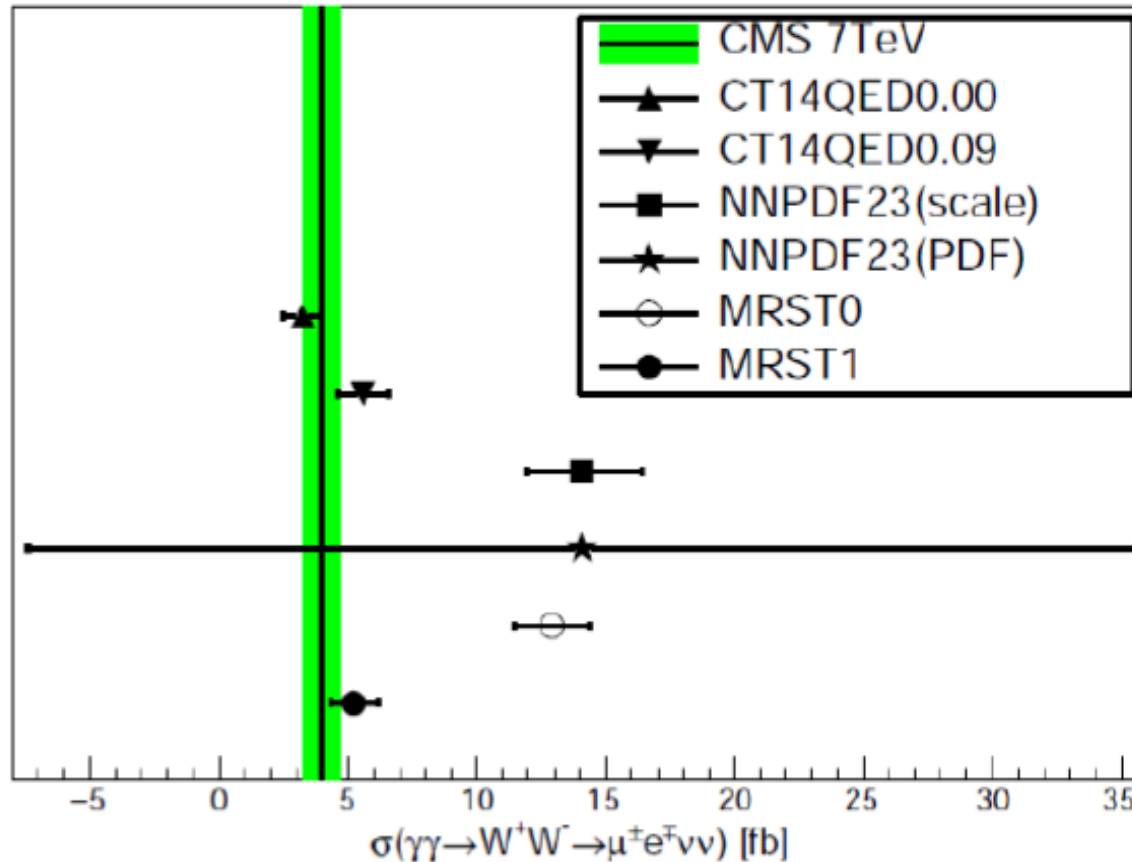






# Compare CMS Data to various photon PDFs

CTEQ



# Bridging Hessian and Monte-Carlo formalisms, and related issues

## Choices of PDF parametrizations

Functional forms, # of parameters. What are associated biases? Are unbiased parametrizations possible?

## Conversion of the Hessian replicas into Monte-Carlo replicas, and back

Several techniques recently developed, e.g., used for the PDF4LHC15 combination

## Definition of PDF uncertainties

### Nature of tolerance $T^2$ on $\chi^2$

What causes the tolerance to increase:

Tensions between experiments? -- partly ( $T \sim 2 - 3$ )

Parametrization dependence?

Hidden theory uncertainties? -- partly ( $T \ll 10$ )

How to choose tolerance without double-counting?

**PDF reweighting techniques:** a promising approach to simplify the fits, but the outcome depends on the assumed replica weights (Giele-Keller vs. NNPDF) and assumed tolerance. What is the right method?

# CT14: new parametrization forms

- CT14 relaxes restrictions on several PDF combinations that were enforced in CT10. [These combinations were not constrained by the pre-LHC data.]
  - The assumptions  $\frac{\bar{d}(x, Q_0)}{\bar{u}(x, Q_0)} \rightarrow 1$ ,  $u_v(x, Q_0) \sim d_v(x, Q_0) \propto x^{A_{1v}}$  with  $A_{1v} \approx -\frac{1}{2}$  at  $x < 10^{-3}$  are relaxed once LHC  $W/Z$  data are included
  - CT14 parametrization for  $s(x, Q)$  includes extra parameters
- CT14 fits have 28 free parameters
- In general,  $f_a(x, Q_0) = Ax^{a_1} (1-x)^{a_2} P_a(x)$
- CT10 assumed  $P_a(x) = \exp(a_0 + a_3\sqrt{x} + a_4x + a_5x^2)$ 
  - exponential form conveniently enforces positive definite behavior
  - but power law behaviors from  $a_1$  and  $a_2$  may not dominate
- In CT14,  $P_a(x) = G_a(x)F_a(z)$ , where  $G_a(x)$  is a smooth factor
  - $z = 1 - 1(1 - \sqrt{x})^{a_3}$  preserves desired Regge-like behavior at low  $x$  and high  $x$  (with  $a_3 > 0$ )
- Express  $F_a(z)$  as a linear combination of Bernstein polynomials:

$$z^4, 4z^3(1-z), 6z^2(1-z)^2, 4z(1-z)^3, (1-z)^4$$

- each basis polynomial has a single peak, with peaks at different values of  $z$ ; reduces correlations among parameters

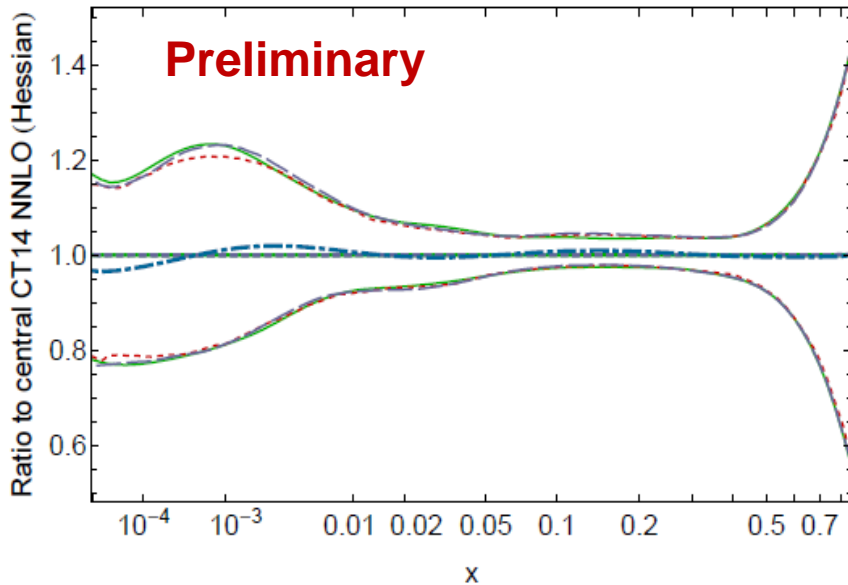
(N+1)-dim. perspective  
eliminates wrong N-dim. solutions



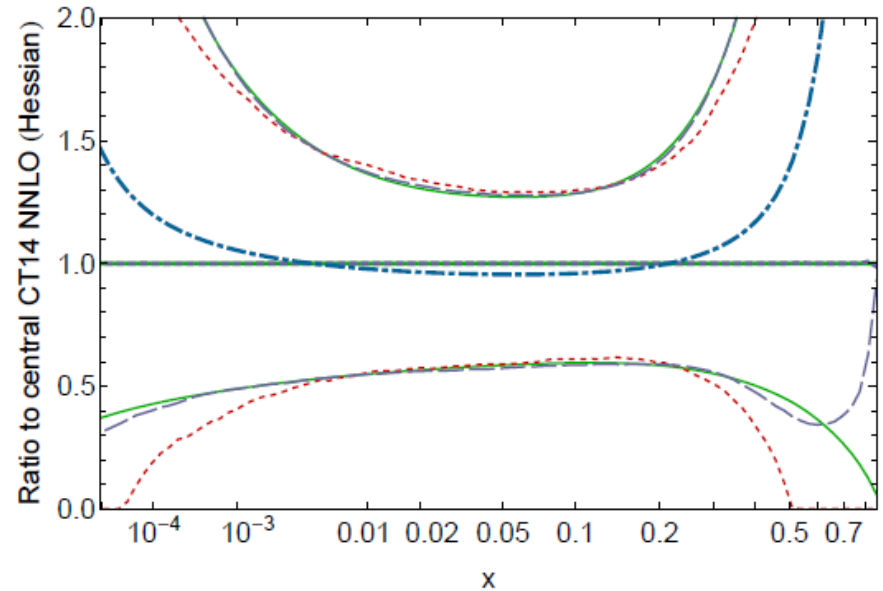
# Comparison of CT14 Hessian and MC asymmetric standard deviations for PDFs (T. J. Hou et al., arXiv:1606.xxxxx)

Watt & Thorne, CTEQ-TEA: Monte-Carlo sampling of Hessian PDFs accounting for asymmetric PDF errors for several underlying probability distributions

$d(x, Q)$  at  $Q=1.3$  GeV, 68% c.l., asym. std. dev.  
CT14 NNLO Hessian (solid), MC (dashed)



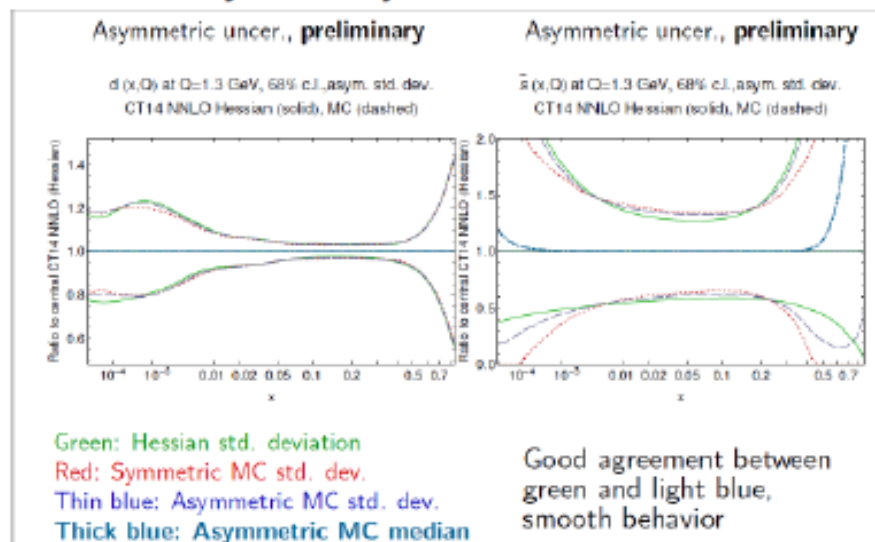
$\bar{s}(x, Q)$  at  $Q=1.3$  GeV, 68% c.l., asym. std. dev.  
CT14 NNLO Hessian (solid), MC (dashed)



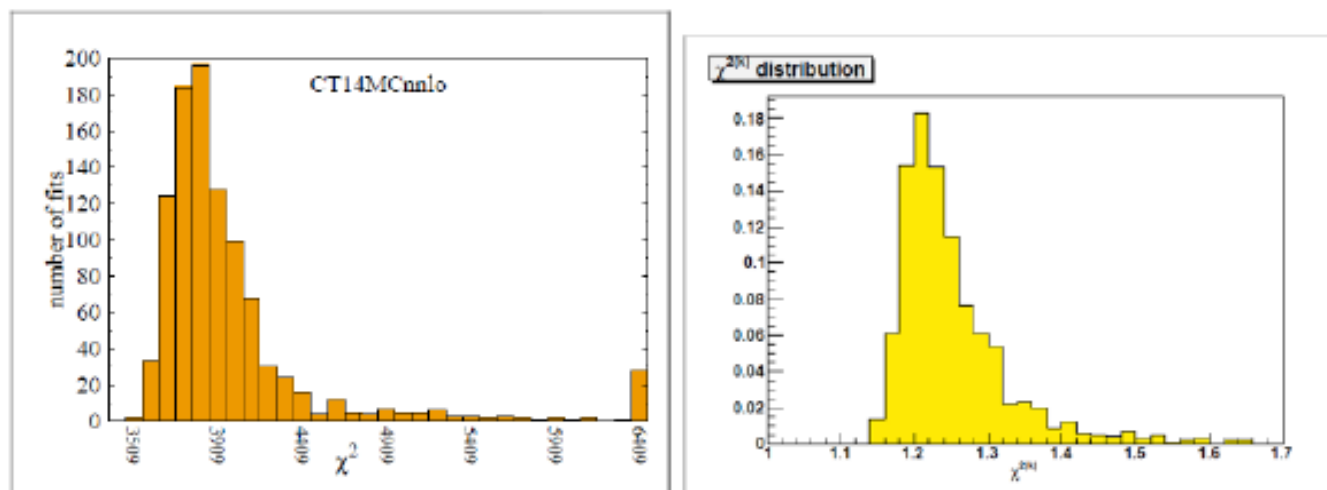
Green: Hessian std. deviation  
Red: Symmetric MC std. dev.  
Thin blue: Asymmetric MC std. dev.  
Thick blue: Asymmetric MC median

Good agreement between green and light blue in central regions, smooth behavior

# CT14 replicas **Hou**. Study of asymmetric uncertainties.



Also plot of  $\chi^2$  distribution for **1000** replicas with **28** eigenvectors and tolerance  $\sim 40$  for one sigma. Extremely similar to **NNPDF** from completely different approach.

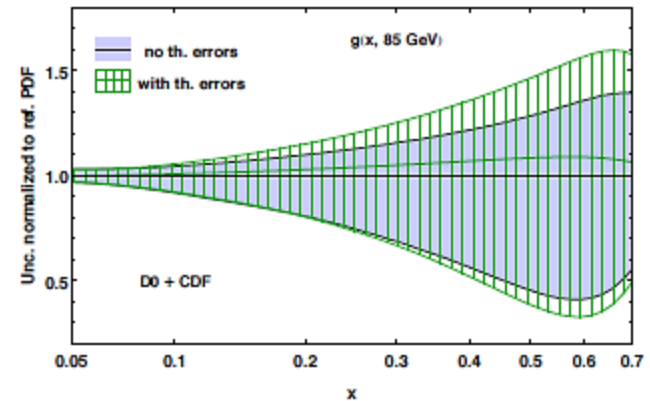


# Residual uncertainty in NLO cross sections

CC DIS and jet production hard cross sections are still computed at NLO

In the CT14 study, we estimate the theoretical uncertainty in the PDFs from the QCD scale dependence and normalization variations in the jet cross sections due to the missing NNLO contributions.

The NLO scale uncertainty in these cases is small compared to the experimental uncertainty.



- ❖ About 20% increase of the gluon PDF uncertainty in large-x region and 10% in the Higgs mass region, for a fit with only Tevatron jet data included (+DIS+...)
- ❖ Similar results are observed when also including the LHC jet data or using different criteria for the determination of PDF uncertainties

Jun Gao,  
2014

## Theoretical accuracy

A variety of comparisons was accomplished to benchmark NNLO theoretical calculations for key scattering processes

1. J. Gao et al., MEKS: a program for computation of inclusive jet cross sections at hadron colliders, arXiv:1207.0513
2. R. Ball et al., Parton Distribution benchmarking with LHC data, arXiv:1211.5142
3. S. Alekhin et al., ABM11 PDFs and the cross section benchmarks in NNLO, arXiv:1302.1516; The ABM parton distributions tuned to LHC data; arXiv:1310.3059
4. A. Cooper-Sarkar et al., PDF dependence of the Higgs production cross section in gluon fusion from HERA data, 2013 Les Houches Proceedings, arXiv:1405.1067, p. 37
5. S. Forte and J. Rojo, Dataset sensitivity of the  $gg \rightarrow H$  cross-section in the NNPDF analysis, arXiv:1405.1067, p. 56

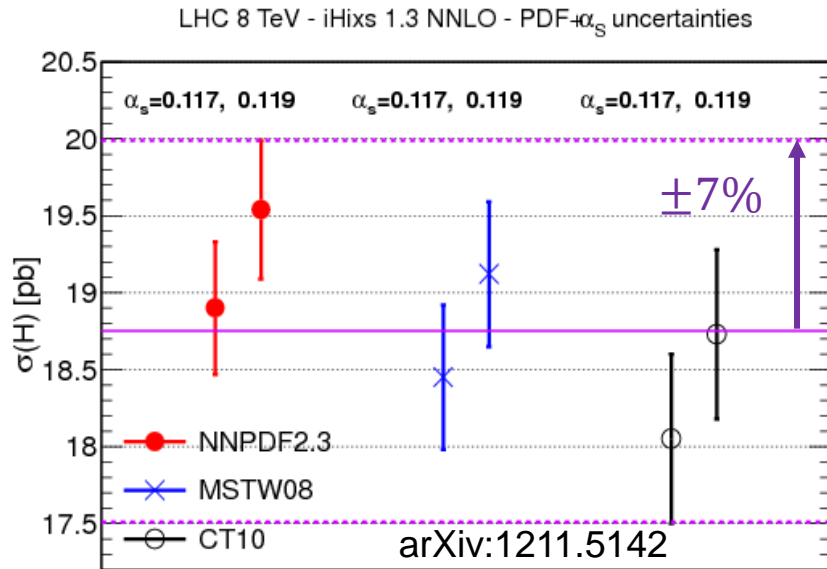
## Verifying statistical methods

**Parametric/Hessian** methodology (CT, MMHT) and **nonparametric/Monte-Carlo methodology** (NNPDF) result in comparable global fits and PDF uncertainties

Advanced PDF parametrizations are employed by CT and MMHT for efficient, minimally biased, extraction of PDFs from global data



# Example: $gg \rightarrow H_{SM}^0$ at the LHC



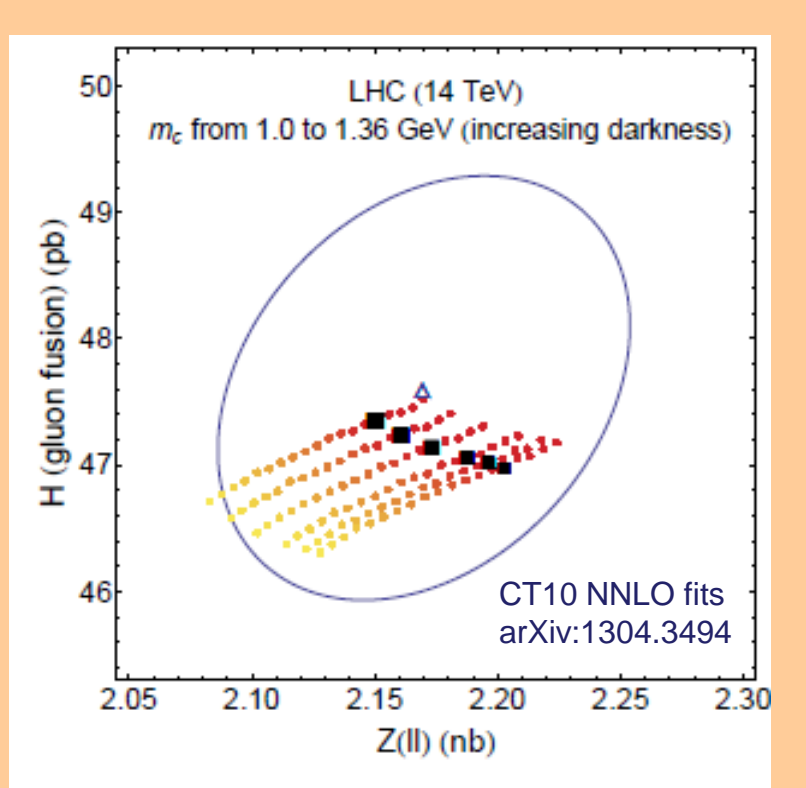
	CT14	MMHT2014	NNPDF3.0
8 TeV	18.66 pb	18.65 pb	18.77 pb
	-2.2%	-1.9%	-1.8%
	+2.0%	+1.4%	+1.8%
13 TeV	42.68 pb	42.70 pb	42.97 pb
	-2.4%	-1.8%	-1.9%
	+2.0%	+1.3%	+1.9%

J.Huston, PDF4LHC, April 2015

For example,  $\delta_{PDF}$  on Higgs cross sections based on 3 **latest** global fits has reduced from 7% to within 3%, i.e., the PDF uncertainty is now of order of N3LO QCD scale uncertainty

This improvement is due to benchmarking of general-mass factorization schemes; but can there be hidden sources of uncertainties on  $\sigma(gg \rightarrow H)$ , e.g., associated with massive charm DIS contributions, cf. arXiv:1603.08906?

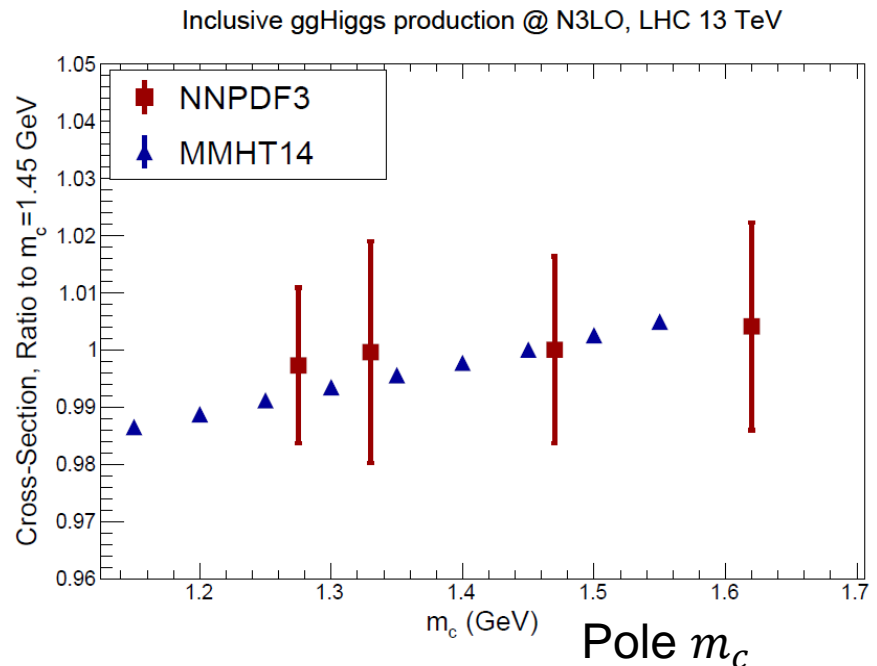
# No. Uncertainty on $\sigma(gg \rightarrow H)$ due to $m_c(m_c)$ is $<2-3\%$



$\sigma_{tot}$  for  $m_c(m_c) = 1 - 1.36$  GeV and matching parameter  $\lambda$  varied independently,  $Q_0 = 1$  GeV. Black boxes are for  $m_c(m_c) = 1.28$  GeV (close to world average), for the explored  $\lambda$ . The error ellipse is for nominal 90% C.L. @  $Q_0 = 1.3$  GeV.

GM-VFN schemes agree well at NNLO because of perturbative convergence, not because of  $m_c$  tuning

Intrinsic charm only reduces correlated dependence on  $m_c$ ,  $Q_0$ , and matching (NNPDF)



# Estimating the PDF+ $\alpha_s$ uncertainty in practical applications

# The Battle Royal



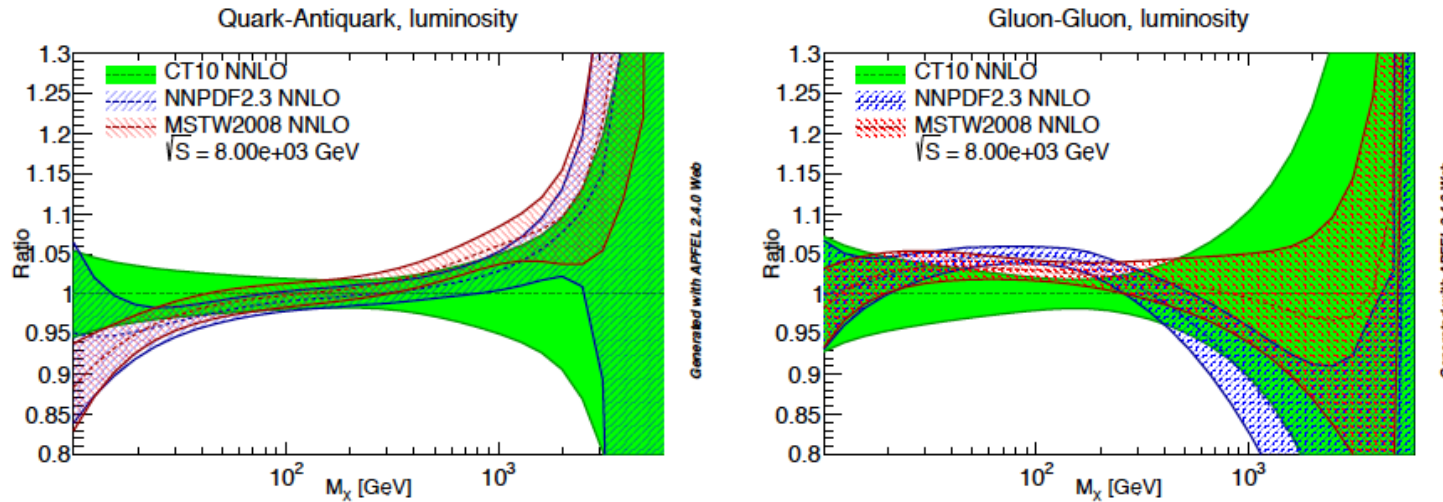
PDF4LHC recommendations  
for LHC Run-II  
(arXIV:1510.03865)



Recommendations for  
PDF usage in LHC  
predictions  
(arXIV:1603.08906)

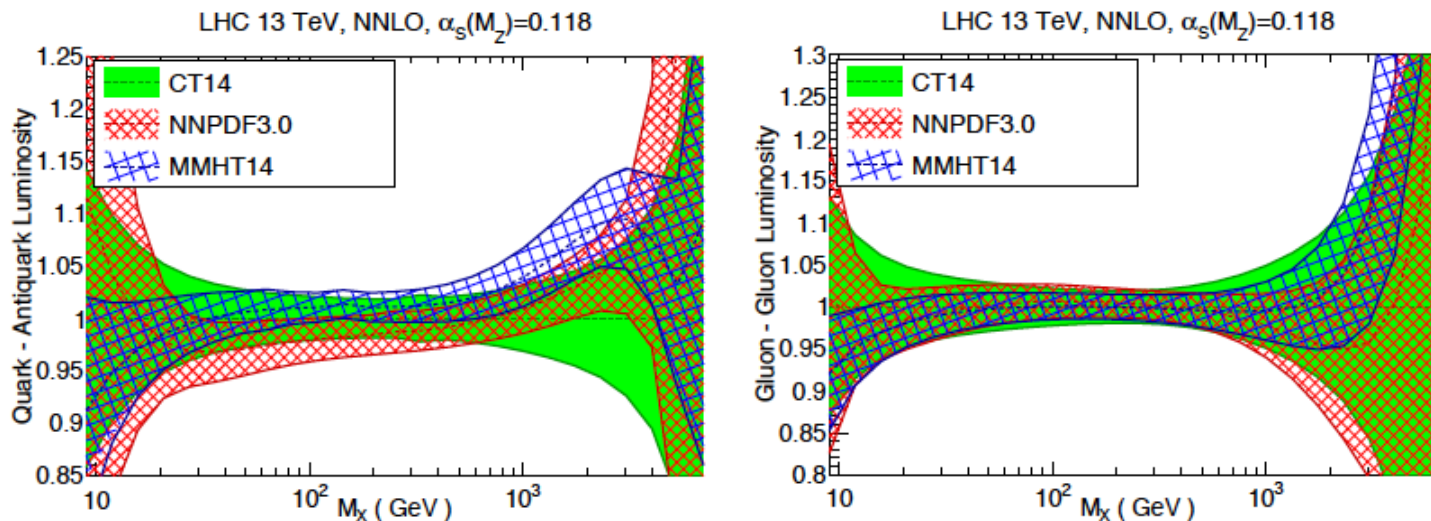
**WHOSE LAW WILL  
PREVAIL?**

# 2012→2015: Agreement between global NNLO PDFs greatly improved



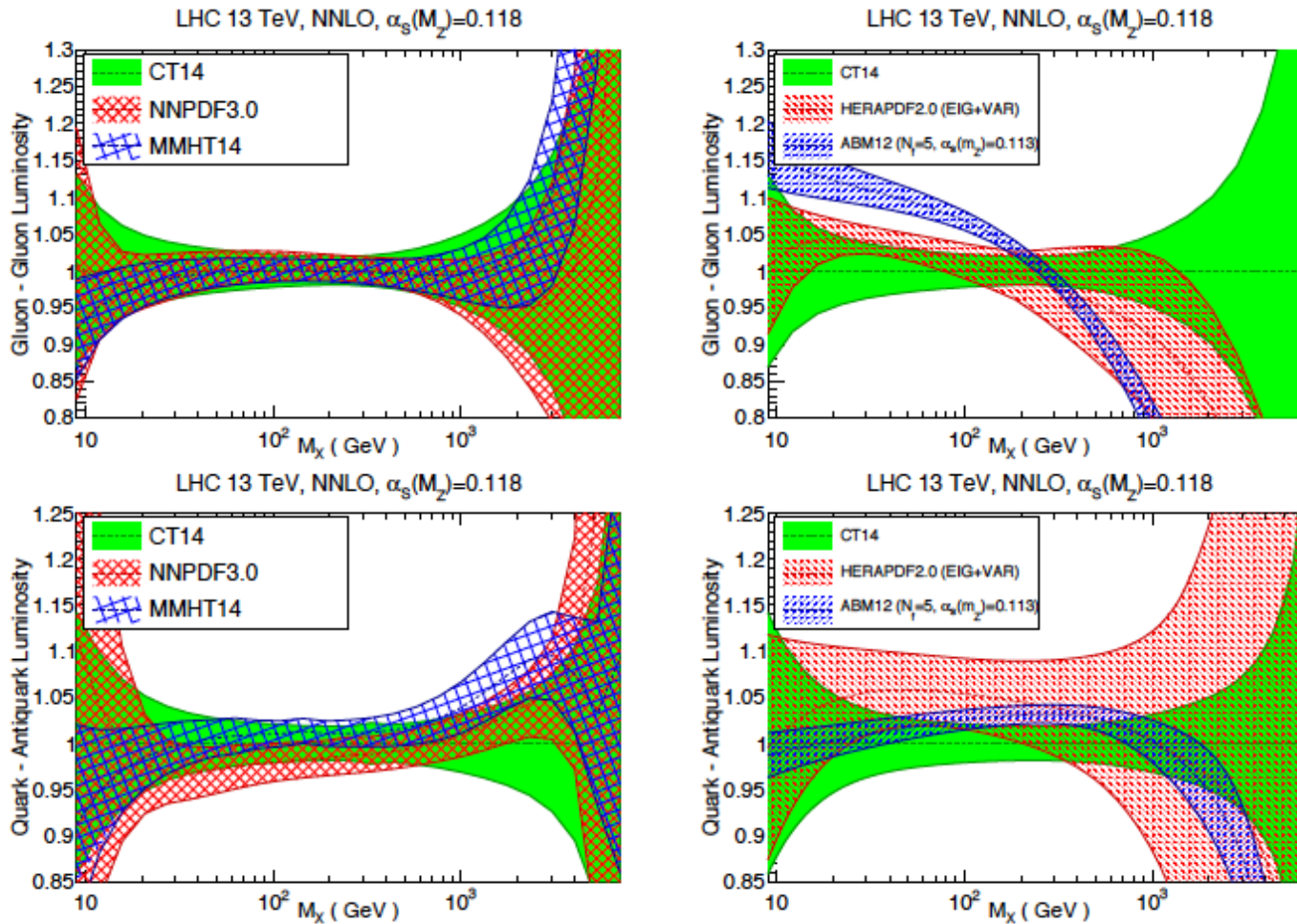
Note in particular the changes in the gg luminosity, especially important in the Higgs mass region

Figure 1: Comparison of the  $q\bar{q}$  (left) and  $gg$  (right) PDF luminosities at the LHC 8 TeV for CT10, MSTW2008 and NNPDF2.3. Results are shown normalized to the central value of CT10.



LHC data has been added for all 3 new PDFs, but most changes are due to benchmarking of formalisms

# ABM'12, HERA2.0 vs. CT14, MMHT14, NNPDF3.0



behavior for  
HERAPDF2.0  
and ABM12  
somewhat  
different

HERAPDF2.0  
uncertainties  
tend to be  
larger

Figure 5: Comparison of the gluon-gluon (upper plots) and quark-antiquark (lower plots) PDF luminosities from the CT14, MMHT14 and NNPDF3.0 NNLO sets (left plots) and from the NNPDF3.0, ABM12 and HERAPDF2.0 NNLO sets (right plots), for a center-of-mass energy of 13 TeV, as a function of the invariant mass of the final state  $M_X$ .

# Given numerous PDF sets, what is the PDF uncertainty in my analysis?

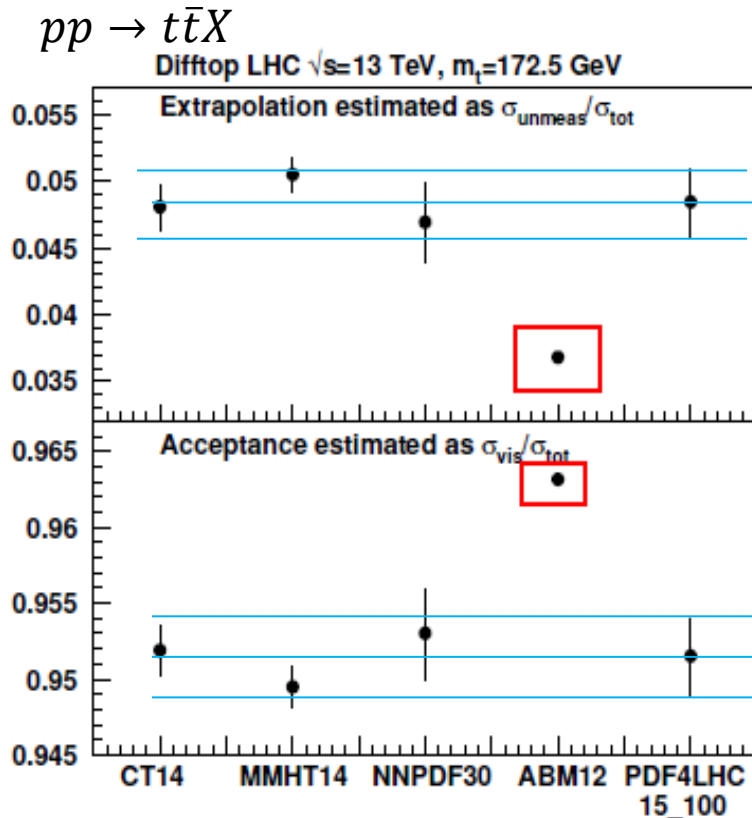


Figure: K. Lipka  
1603.08906

The procedure for computing the PDF uncertainty must vary depending on the goals. The options may include

- Using one individual set out of several similar ones (e.g., CT, MMHT, or NNPDF)
- Using an envelope of all sets, including the outlier sets
- 2015 recommendation by the PDF4LHC working group** (arXiv:1510.03865):

- Several procedures spelled out for computation of PDF uncertainties, depending on the context
- Estimation of PDF uncertainties is streamlined in many cases by using combined PDF4LHC15 sets based on CT14, MMHT14, and NNPDF3.0

## PDF4LHC recommendations for LHC Run II

Jon Butterworth<sup>1</sup>, Stefano Carrazza<sup>2</sup>, Amanda Cooper-Sarkar<sup>3</sup>, Albert De Roeck<sup>4,5</sup>, Joël Feltesse<sup>6</sup>, Stefano Forte<sup>2</sup>, Jun Gao<sup>7</sup>, Sasha Glazov<sup>8</sup>, Joey Huston<sup>9</sup>, Zahari Kassabov<sup>2,10</sup>, Ronan McNulty<sup>11</sup>, Andreas Morsch<sup>4</sup>, Pavel Nadolsky<sup>12</sup>, Voica Radescu<sup>13</sup>, Juan Rojo<sup>14</sup> and Robert Thorne<sup>1</sup>.

**A major revision of the  
previous PDF4LHC  
recommendation in  
arxiv:1101.0538,  
arXiv:1211.5142**

**+ 2 follow-up  
contributions in 2015  
Les Houches  
proceedings**

Read for detailed  
suggestions on selecting  
and using PDFs in various  
situations





# PDF4LHC publication, topics

1. Review of updates on PDFs from various groups

**NNLO Global PDF sets:** CT14, MMHT'14, NNPDF3

**PDFs using other methodologies:** ABM'12, CJ15, HERAPDF2.0



2. Average PDF sets by PDF4LHC group: PDF4LHC15\_30, \_100, \_MC

Criteria for combination

$$\alpha_s(M_Z) = 0.1180 \pm 0.0015 \text{ at 68\% c.l.}$$

3. Recommendation on selecting PDF sets for various LHC applications

A. New physics searches

B. Precision tests of SM and PDFs

C. Monte-Carlo simulations

D. Acceptance estimates

Average PDF sets **can** be used for **bulk of applications** in A, C, D

# Now on LHAPDF:

NLO, NNLO, varied  $\alpha_s$  sets  
 $N_f = 5$  and 4 (upcoming)

LHAPDF6 grid	Pert order	ErrorType	$N_{\text{mem}}$	$\alpha_s(m_Z^2)$
PDF4LHC15_nnlo_mc	NNLO	replicas	100	0.118
PDF4LHC15_nnlo_100	NNLO	symmhessian	100	0.118
PDF4LHC15_nnlo_30	NNLO	symmhessian	30	0.118
PDF4LHC15_nnlo_mc_pdfas	NNLO	replicas+as	102	mem 0:100 $\rightarrow$ 0.118 mem 101 $\rightarrow$ 0.1165 mem 102 $\rightarrow$ 0.1195
PDF4LHC15_nnlo_100_pdfas	NNLO	symmhessian+as	102	mem 0:100 $\rightarrow$ 0.118 mem 101 $\rightarrow$ 0.1165 mem 102 $\rightarrow$ 0.1195
PDF4LHC15_nnlo_30_pdfas	NNLO	symmhessian+as	32	mem 0:30 $\rightarrow$ 0.118 mem 31 $\rightarrow$ 0.1165 mem 32 $\rightarrow$ 0.1195
PDF4LHC15_nnlo_asvar	NNLO	-	1	mem 0 $\rightarrow$ 0.1165 mem 1 $\rightarrow$ 0.1195

Table 5: Summary of the combined NNLO PDF4LHC15 sets with  $n_f^{\text{max}} = 5$  that are available from LHAPDF6. The corresponding NLO sets are also available. Members 0 and 1 of PDF4LHC15\_nnlo\_asvar coincide with members 101 and 102 (31 and 32) of PDF4LHC15\_nnlo\_mc\_pdfas and PDF4LHC15\_nnlo\_100\_pdfas (PDF4LHC15\_nnlo\_30\_pdfas). Recall that in LHAPDF6 there is always a zeroth member, so that the total number of PDF members in a given set is always  $N_{\text{mem}} + 1$ . See text for more details.

# Averaging of PDF ensembles

The 2012 recommendation estimated the combined uncertainty as an envelope of **cross sections** for 3 PDF sets; the envelope was overly sensitive to outliers

By 2015, several methods for combination (averaging) of **PDFs** (before computing cross sections) were developed. Criteria allowing the combination were outlined.

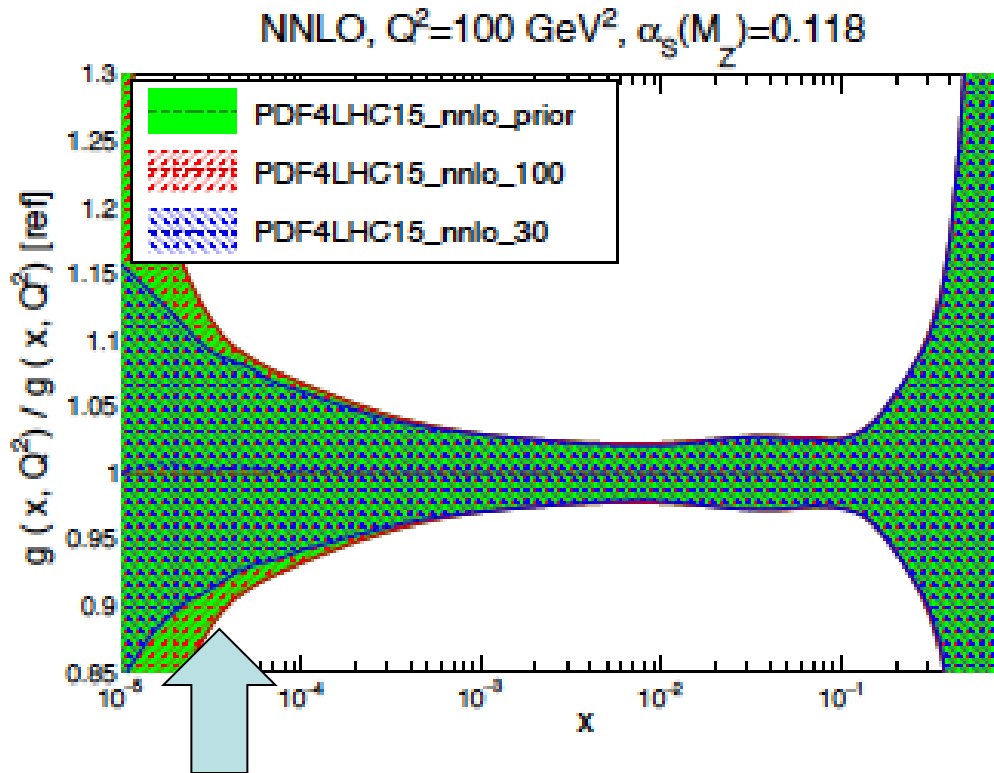
## Combination workflow:

1. Generate 900 MC replicas from all input ensembles (currently CT14, MMHT14, NNPDF3.0) using Thorne-Watt procedure
  - Other PDF sets can be added in the future if they satisfy the listed criteria
2. Reduce the number of final replicas from 900 to 100 or 30 by keeping most relevant PDF combinations

# Reduced sets

- 900 error PDFs are too much for general use
- 3 reduction techniques have been developed
  - Compressed Monte Carlo PDFs (PDF4LHC15\_nnlo(nlo)\_mc)
    - 100 PDF error sets; preserve non-Gaussian errors
  - **META Hessian PDFs (PDF4LHC15\_nnlo(nlo)\_30)**
    - 30 PDF error sets using METAPDF technique; Gaussian (symmetric) errors
  - MCH Hessian PDFs (PDF4lhc15\_nnlo(nlo)\_100)
    - 100 PDF error sets using MCH technique; Gaussian (symmetric errors)
- The META technique is able to more efficiently reproduce the uncertainties when using a limited number (30) of error PDFs
- The MCH technique best reproduces the uncertainties of the 900 MC set prior

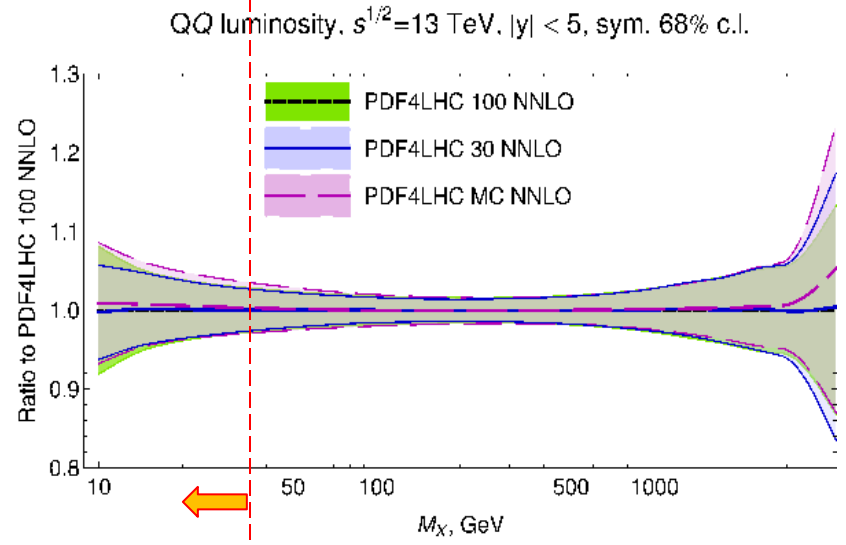
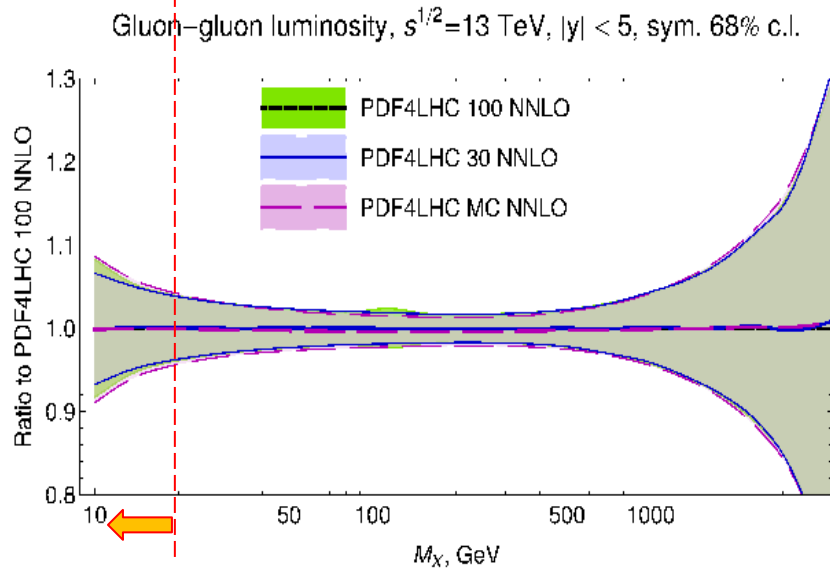
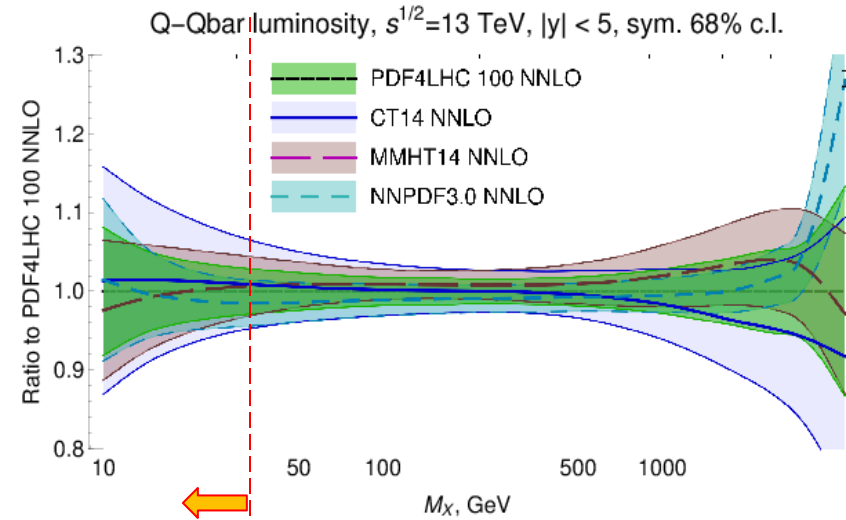
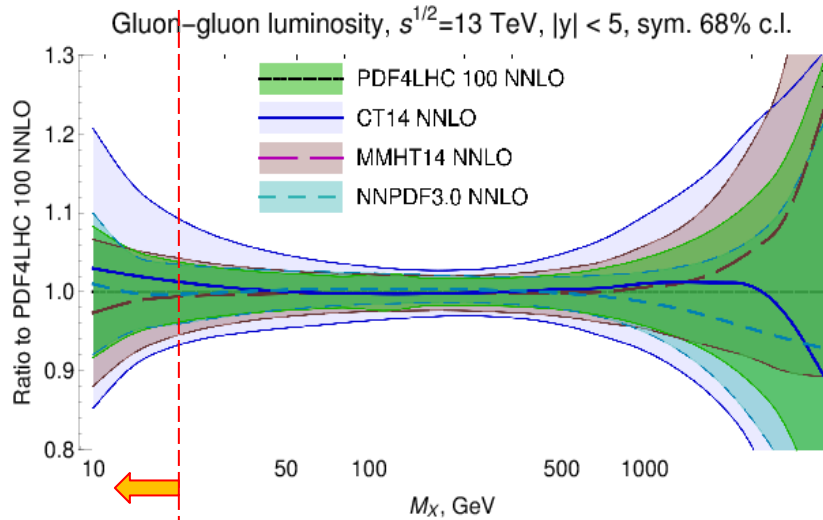
# Comparisons of ensembles with 900, 100, 30 replicas



Three reduced PDF4LHC sets (100, MC, 30) reproduce well the 900-replica prior. Keep in mind that the uncertainty of the prior has an uncertainty of its own. By their construction, the lowest Hessian eigenvector sets are known the best, the highest sets are known with less confidence.

The 30-member ensemble keeps the lowest, best known sets and thus provides a lower estimate for the \_900 prior uncertainty, known with higher confidence. When this estimate is not sufficient, or non-Gaussianities are important, use the 100 and MC sets

# Ranges with differences between input PDFs, prior, and reduced sets



5/23/2016

P. Nadolsky, KITP UCSB

Note the  $|y| < 5$  cut to constrain comparisons to the experimentally accessible region 46

# Dependence of LHC observables on parton distribution functions

## CONTENTS

### 1. $p + p \rightarrow Z + X$

- [settings of the calculation] [Applgrid files]
- PDF4LHC15 PDFs (NLO)
- PDF4LHC15 PDFs (NNLO)
- PDF4LHC15\_100, HERA, ABM PDFs (NNLO)
- PDF4LHC15\_100, CT14, MMTH14, NNPDF3.0 PDFs (NNLO)

### 2. $p + p \rightarrow W^+ + X$

- [settings of the calculation] [Applgrid files]
- PDF4LHC15 PDFs (NLO)
- PDF4LHC15 PDFs (NNLO)
- PDF4LHC15\_100, HERA, ABM PDFs (NNLO)

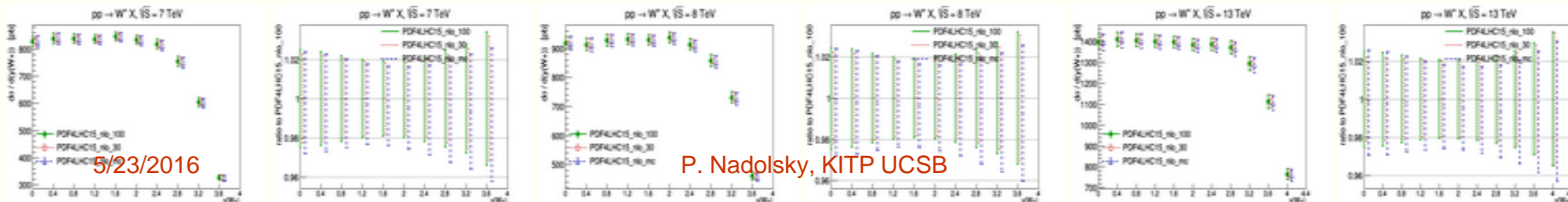
**META gallery for basic processes at 7, 8, 13 TeV**

Developed by Bo Ting Wang and Keeping Xie

### $p + p \rightarrow W^+ + X$

[settings of the calculation] [Applgrid files]

PDF4LHC15 PDFs (NLO)



P. Nadolsky, KITP UCSB

5/23/2016

[pdf] [eps] [pdf] [eps] [pdf] [eps] [pdf] [eps] [pdf] [eps] [pdf] [eps]

# Gallery of phenomenological comparisons for LHC

Process	Order	Type of calculation
• $p + p \rightarrow Z + X$	NLO	aMCFast/APPLgrid
• $p + p \rightarrow W^+ + X$	NLO	aMCFast/APPLgrid
• $p + p \rightarrow W^- + X$	NLO	aMCFast/APPLgrid
• $p + p \rightarrow t\bar{t} + X$	NLO	aMCFast/APPLgrid
• $p + p \rightarrow t\bar{t} + X$	NLO	aMCFast/APPLgrid
• $p + p \rightarrow t\bar{t}\gamma + X$	NLO	aMCFast/APPLgrid
• ATLAS inclusive jets	NLO	NLOJET++/APPLgrid
• ATLAS inclusive dijets	NLO	NLOJET++/APPLgrid
• $P + p \rightarrow W^+ c + X$	NLO	aMCFast/APPLgrid
• $P + p \rightarrow W^- c + X$	NLO	aMCFast/APPLgrid
• $P + p \rightarrow H + X$	LO, NLO	MCFM
• $P + p \rightarrow H + \text{jet} + X$	LO, NLO	MCFM

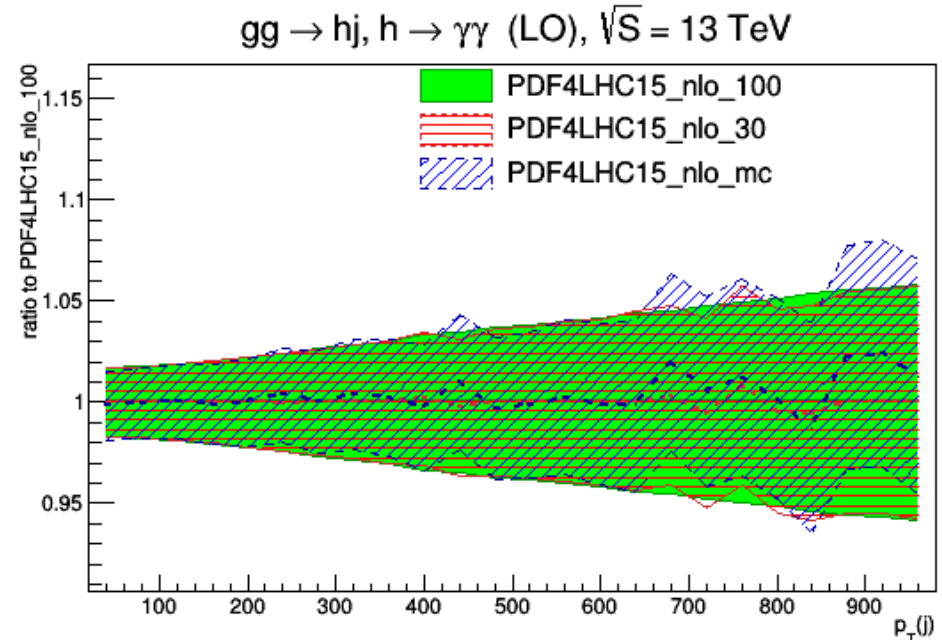
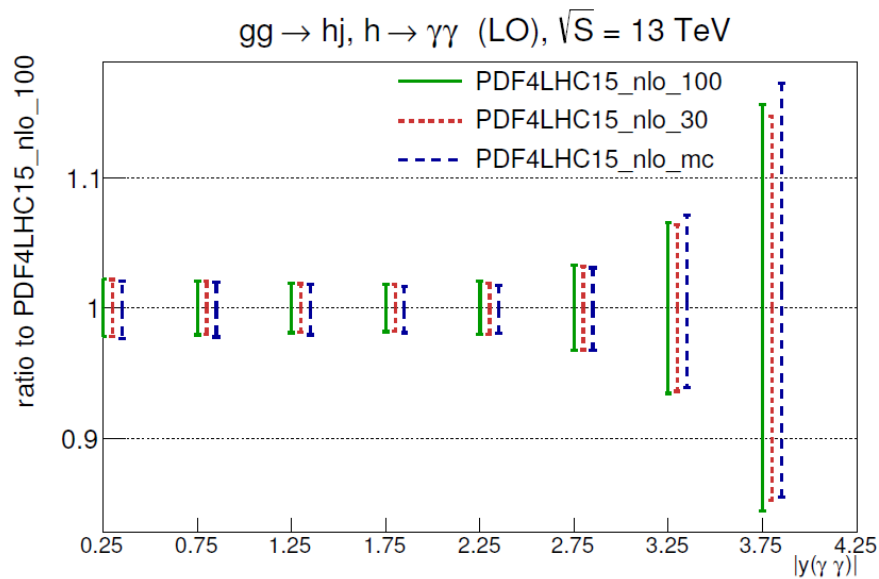
Compared PDFs: PDF4LHC15\_100, \_30, \_MC, ABM'12, CT14, HERA2.0, MMHT14, NN3.0

Both full (MCFM) and fast (AppGrid) calculations. AppGrids are generated with minimal cuts and can be downloaded.



# MCFM: compare PDF and Monte-Carlo integration errors

## Differences of PDF4LHC PDFs matter only when MC errors are negligible

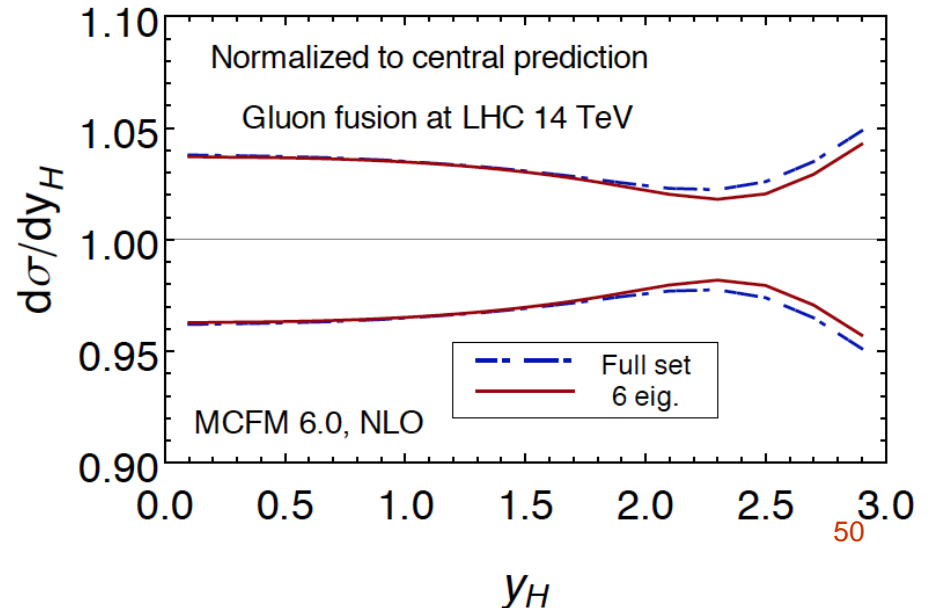
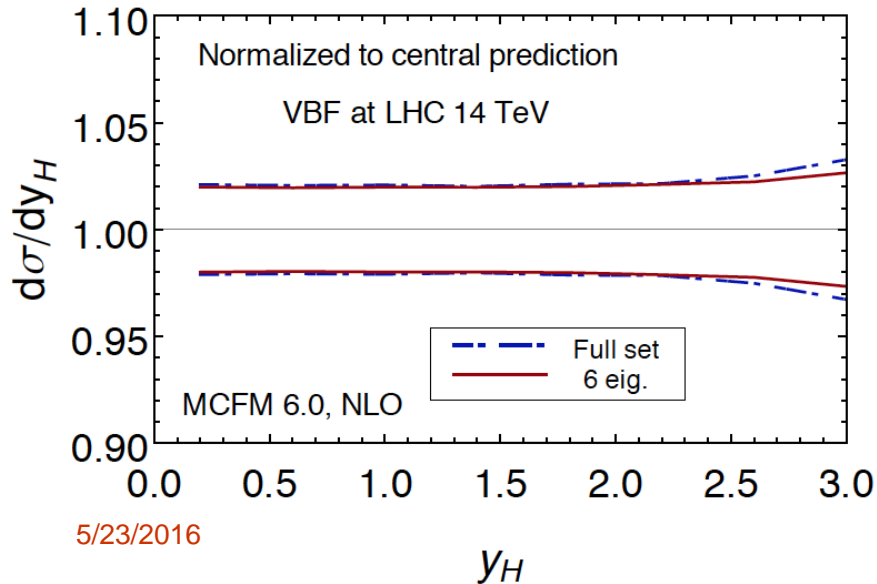
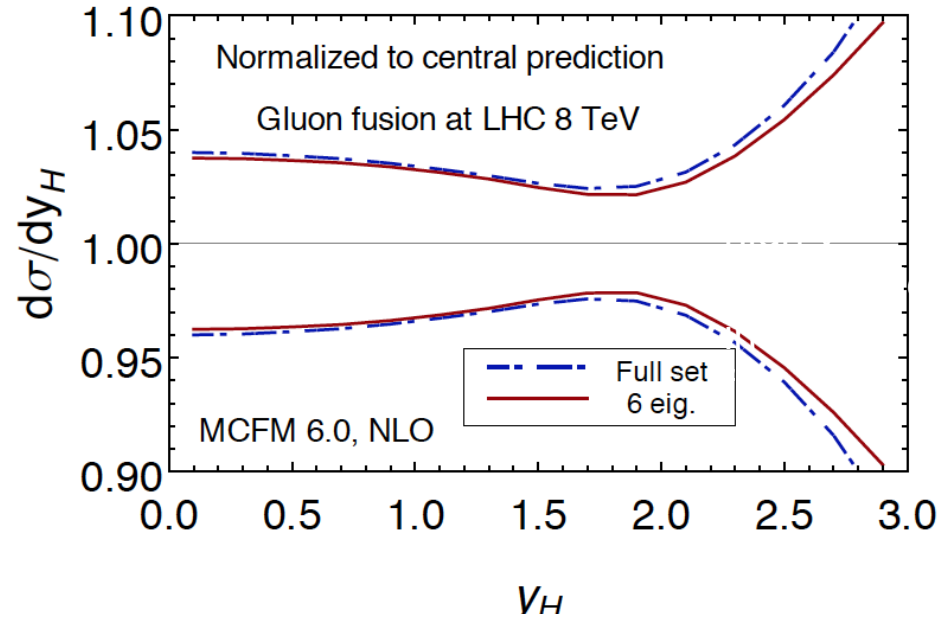


*gg*  $\rightarrow$  *H* + *j* at LO.  
 $10^6$  events,  $\sim 1$  hour per  
each PDF family

MC fluctuations in **central values** and PDF errors are often of the same order as the primordial differences

# Higgs eigenvector set

- For a given class of observables, the `_30` set can be **diagonalized** to reproduce the bulk of the uncertainties and correlations with  $\sim 6$  eigenvector sets



process	$\sigma_{cen.}$	$\delta_{Full}$	$\delta_{Diag.}$	$\sigma_{0.116}^{\alpha_s}$	$\sigma_{0.12}^{\alpha_s}$
$gg \rightarrow H$ [pb]	18.77	+0.48 -0.46	+0.48 -0.44	18.11	19.4
	43.12	+1.13 -1.07	+1.13 -1.04	41.68	44.6
VBF [fb]	302.5	+7.8 -6.7	+7.6 -6.7	303.1	301.4
	878.2	+19.7 -17.9	+19.2 -17.3	877.3	878.2
$HZ$ [fb]	396.3	+8.4 -7.3	+8.1 -7.4	393.0	399.1
	814.3	+14.8 -13.2	+13.8 -13.0	806.5	823.2
$HW^\pm$ [fb]	703.0	+14.4 -14.4	+14.3 -14.1	697.4	708.9
	1381	+28 -22	+26 -22	1368	1398
$HH$ [fb]	7.81	+0.33 -0.30	+0.33 -0.30	7.50	8.10
	27.35	+0.78 -0.72	+0.78 -0.68	26.48	28.2
$t\bar{t}$ [pb]	248.4	+9.1 -8.2	+9.2 -8.1	237.1	259.1
	816.9	+21.4 -19.6	+21.4 -18.4	785.5	848.2
$Z/\gamma^*(l^+l^-)$ [nb]	1.129	+0.025 -0.023	+0.024 -0.023	1.113	1.14
	1.925	+0.043 -0.041	+0.040 -0.037	1.897	1.95
$W^+(l^+\nu)$ [nb]	7.13	+0.14 -0.14	+0.14 -0.13	7.03	7.25
	11.64	+0.24 -0.23	+0.22 -0.21	11.46	11.8
$W^-(l^-\bar{\nu})$ [nb]	4.99	+0.12 -0.12	+0.12 -0.11	4.92	5.08
	8.59	+0.21 -0.20	+0.19 -0.18	8.46	8.74
$W^+W^-$ [pb]	4.14	+0.08 -0.08	+0.08 -0.07	4.04	4.20
	7.54	+0.15 -0.14	+0.14 -0.12	7.39	7.57
$ZZ$ [pb]	0.703	+0.016 -0.014	+0.015 -0.014	0.695	0.71
	1.261	+0.026 -0.024	+0.024 -0.022	1.256	1.27
$W^+Z$ [pb]	1.045	+0.019 -0.018	+0.019 -0.017	1.039	1.06
	1.871	+0.033 -0.031	+0.029 -0.027	1.850	1.89
$W^-Z$ [pb]	0.788	+0.020 -0.019	+0.019 -0.018	0.780	0.79
	1.522	+0.034 -0.032	+0.033 -0.031	1.509	1.54

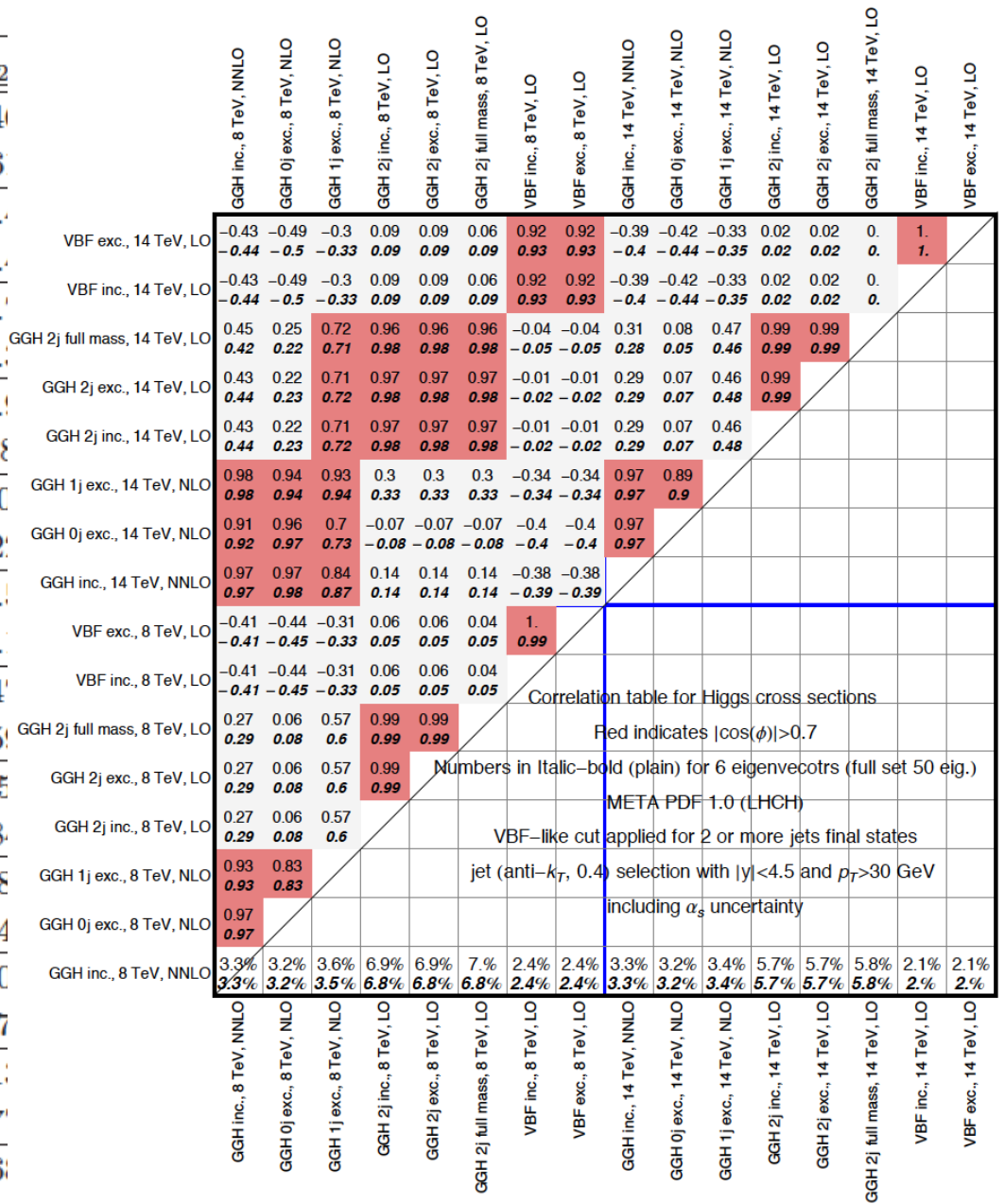


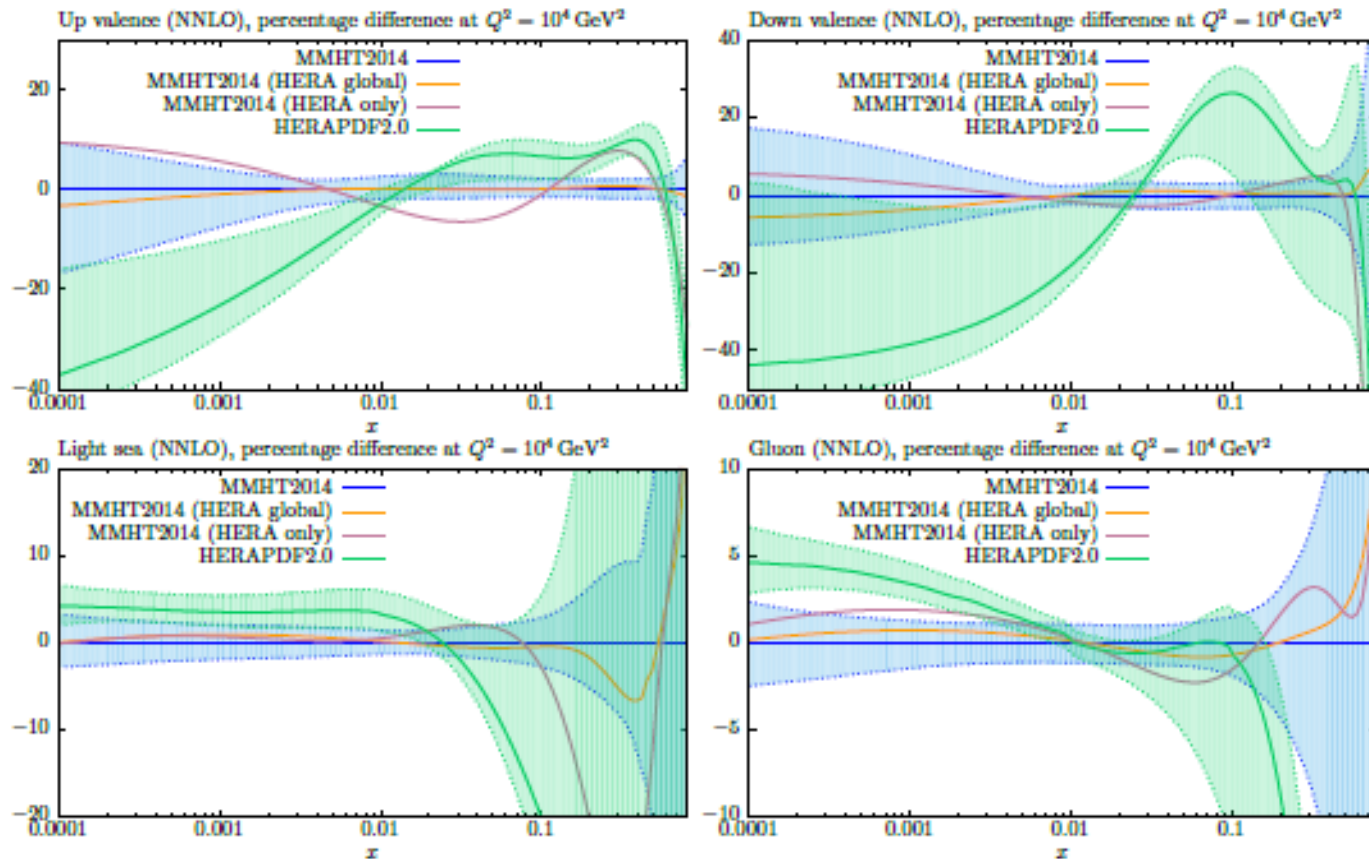
FIG. 7: Same as Fig. 5, with  $\alpha_s$  uncertainties included by adding in quadrature.



# NOW I AM READY FOR QUESTIONS

# Backup slides

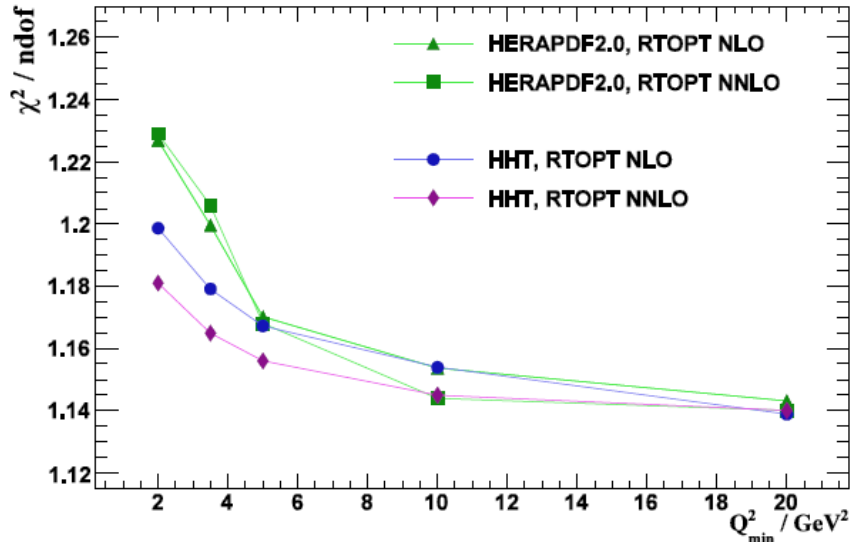
MMHT refit including combined HERA I+II data. Under refitting in global fit NLO –  $\chi^2 = 1533/1185 = 1.29$  per point. NNLO –  $\chi^2 = 1457/1185 = 1.23$  per point.



HERA II modified PDFs very well within MMHT2014 uncertainties. PDFs from HERA II data only fit in some ways similar to HERAPDF2.0.

# Modifications to the HERAPDF2.0 fit called HHT

By I.Abt, **A.M.Cooper-Sarkar**, B.Foster, V.Myronenko, K.Wichmann, M.Wing

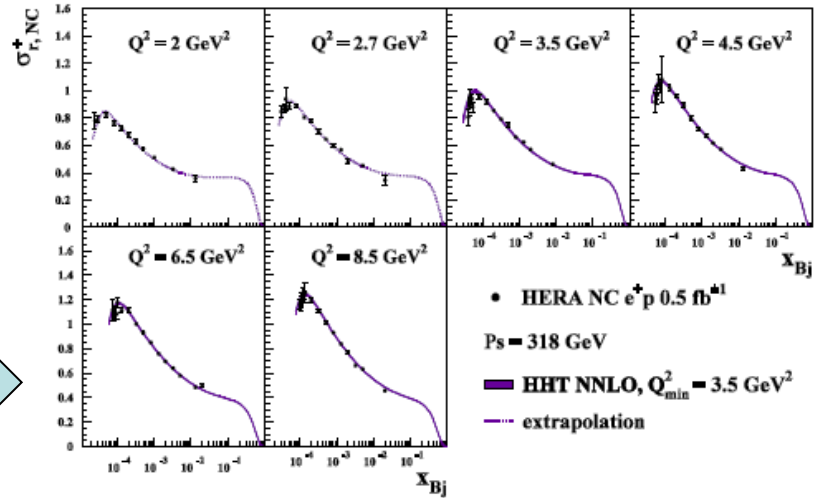
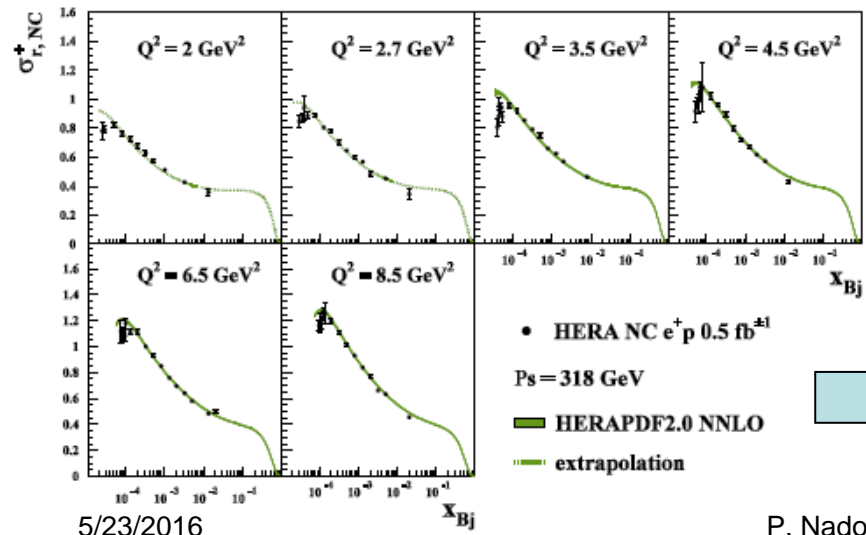


$$F_{2,L} = F_{2,L} (1 + A_{2,L}^{HT}/Q^2)$$

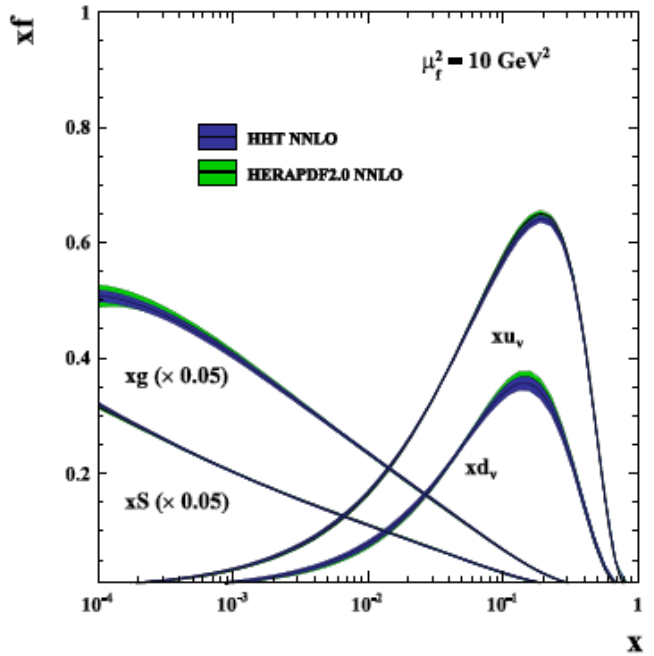
Addition of Higher Twist terms

- requires only modification of  $F_L$
- and is only important for low-x

Greatly improves the description of low- $Q^2$ , low-x and high-y data particularly at NNLO

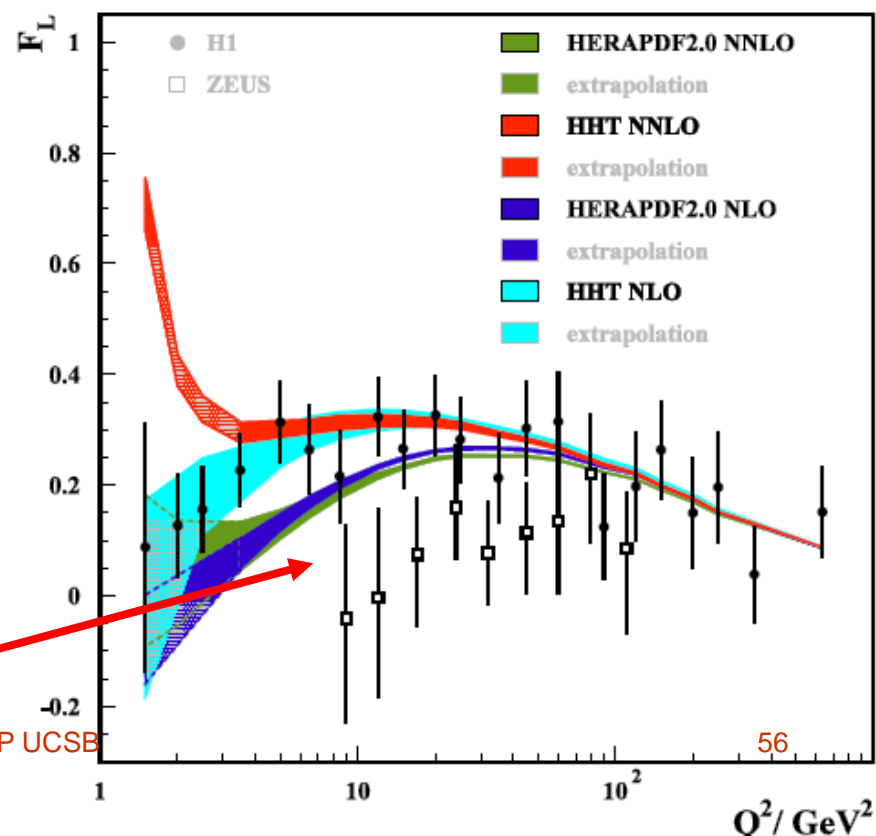


PDFs – and hence high  $Q^2$  physics - not changed



Predicted FL - compared to the measured FL from H1 and ZEUS – is enhanced for  $Q^2 < 50 \text{ GeV}^2$ .

However it is clear that this approach cannot be pushed to very low  $Q^2 < \sim 2 \text{ GeV}^2$



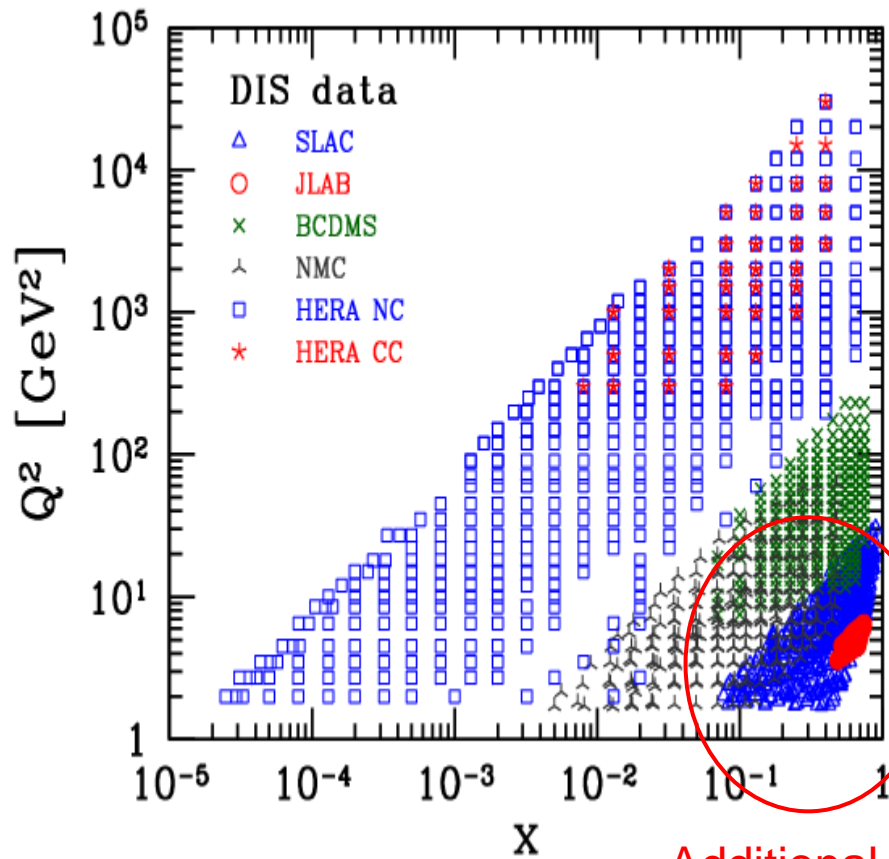
**P.N.:** Notice differences between H1 and ZEUS

P. Nadolsky, KITP UCSB



# Specialized PDF sets

# CJ15: DIS data for $Q^2 > 1.3 \text{ GeV}^2$ , $W^2 > 3 \text{ GeV}^2$



Additional constraints on  $d/u$

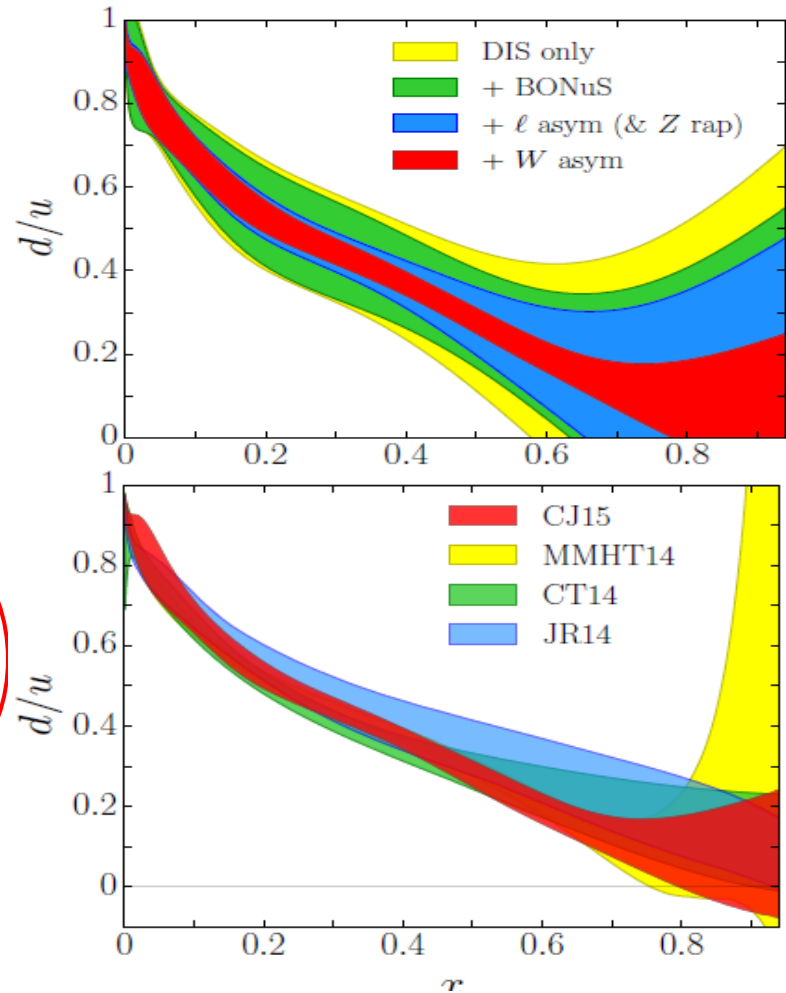
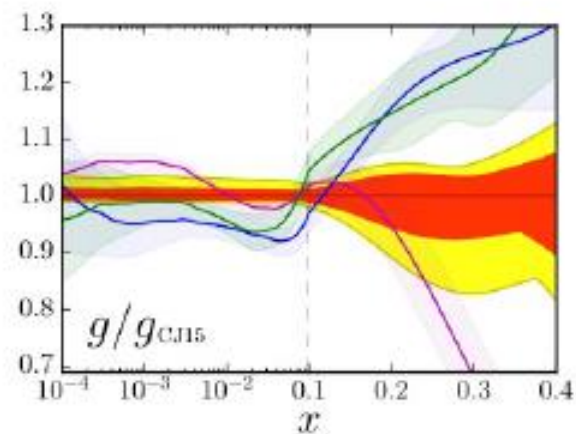
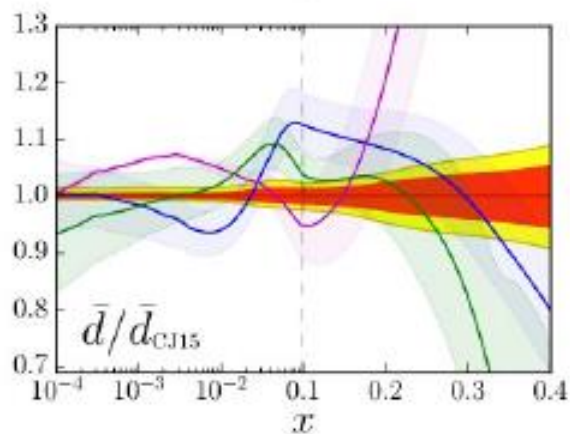
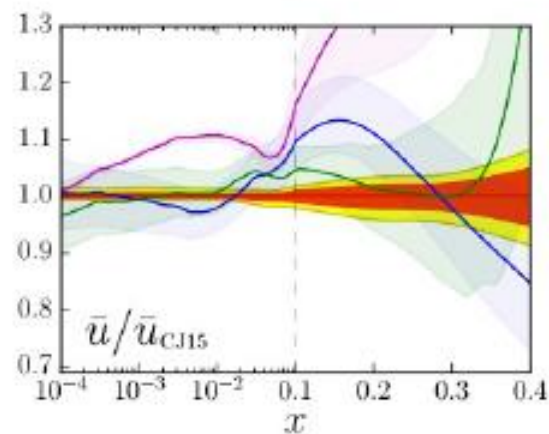
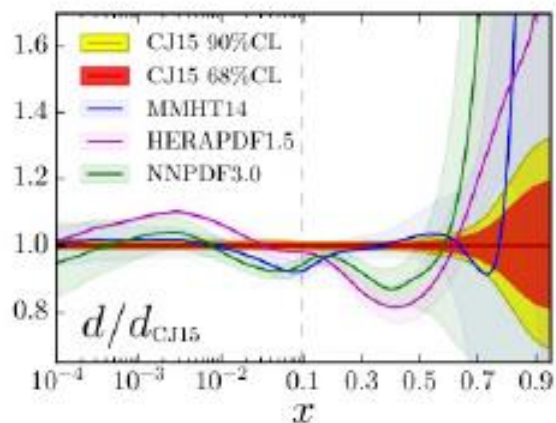
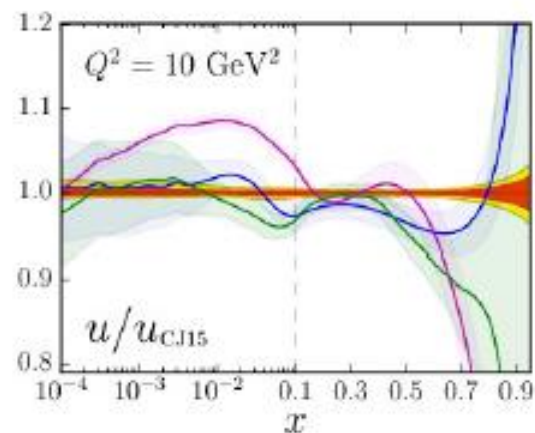


FIG. 16: Comparison of the  $d/u$  ratio at  $Q^2 = 10 \text{ GeV}^2$  for different PDF parametrizations: CJ15 (red band), MMHT14 [6] (yellow band), CT14 [7] (green band), and JR14 [10] (blue band).

# CJ15 vs. others



# Intrinsic Charm PDFs from CTEQ-TEA Global Analysis

S. Dulat et al., 1309.0025; PoS DIS2015 (2015) 166

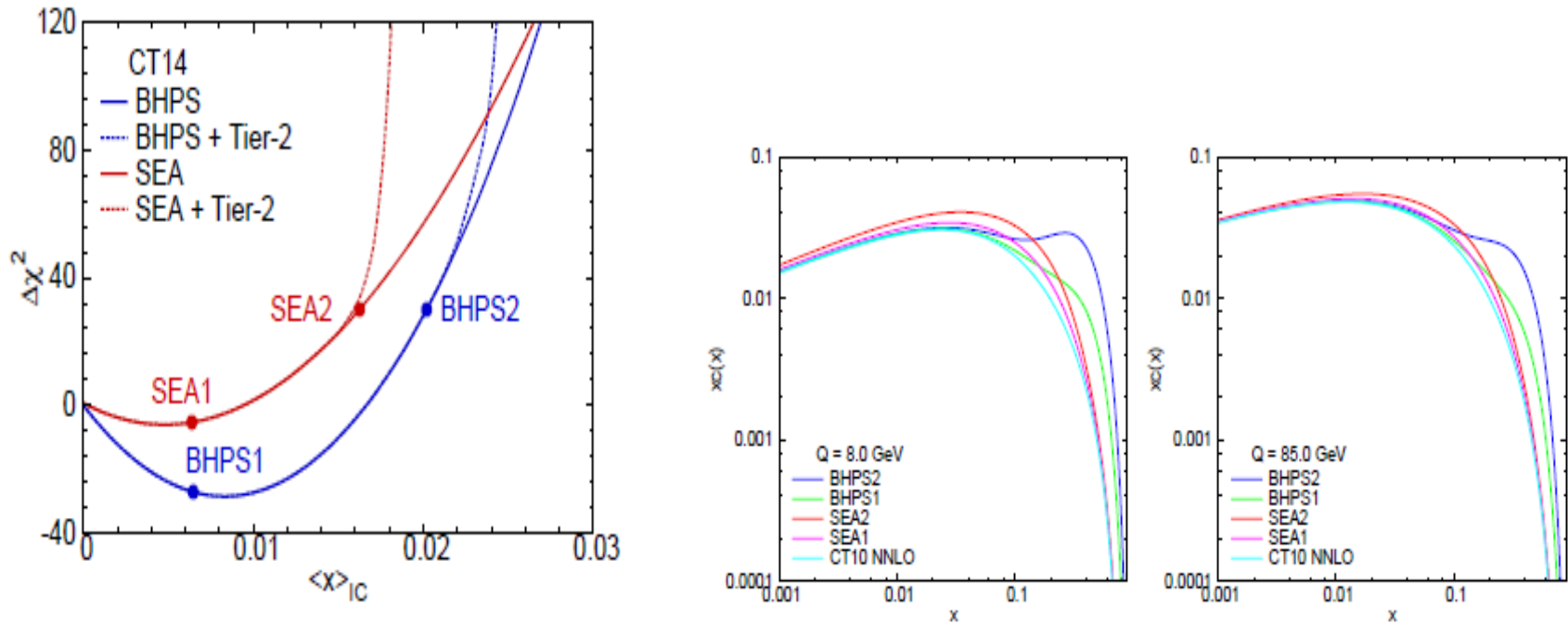
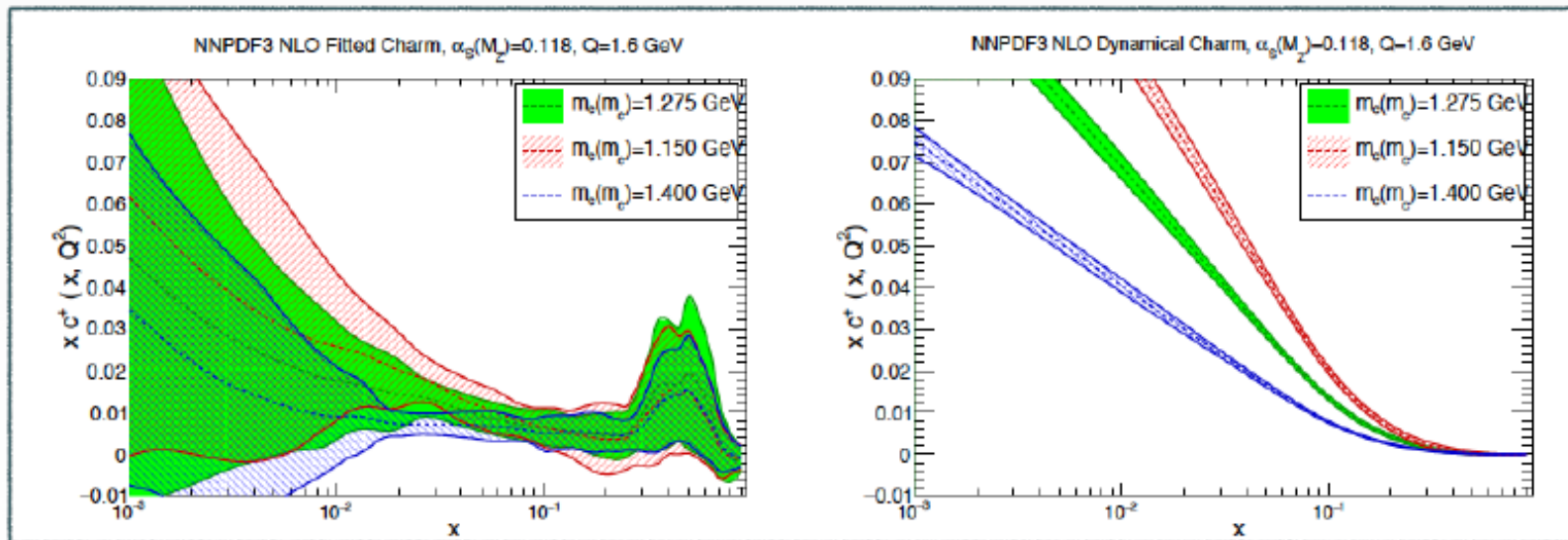


Figure 1: The  $\Delta\chi^2$  versus the momentum fraction of charm  $\langle x \rangle_{IC}$ .

3. 3: Charm quark distribution  $x c(x, Q)$  from the BHPS1 and BHPS2 PDFs (which have 0.57% and 2%  $\langle x \rangle_{IC}$ ); from SEA1 and SEA2 PDFs (which have 0.57% and 1.5%  $\langle x \rangle_{IC}$ ); and from CT10.

# News from NNPDF (II)

- First determination of the **fitted charm PDF** in the NNPDF framework
- **Non-perturbative charm** can account for **up to 0.8%** of the proton momentum (68% CL)
- The EMC charm structure function data can be satisfactorily described
- Fitting the charm PDF stabilises the  $m_c$  dependence of **high-scale cross-sections**

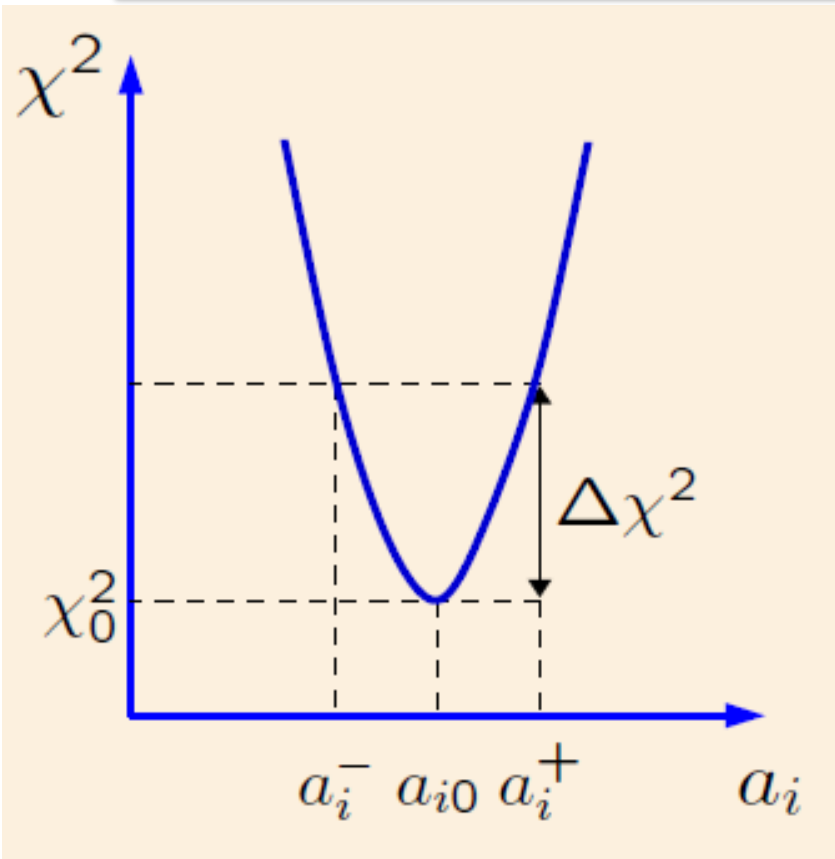


*More in the talks from Juan Rojo (Tue) and Luca Rottoli (Wed)*

# Origin of increased tolerance

# Error analysis: unique parametric model, compatible experiments

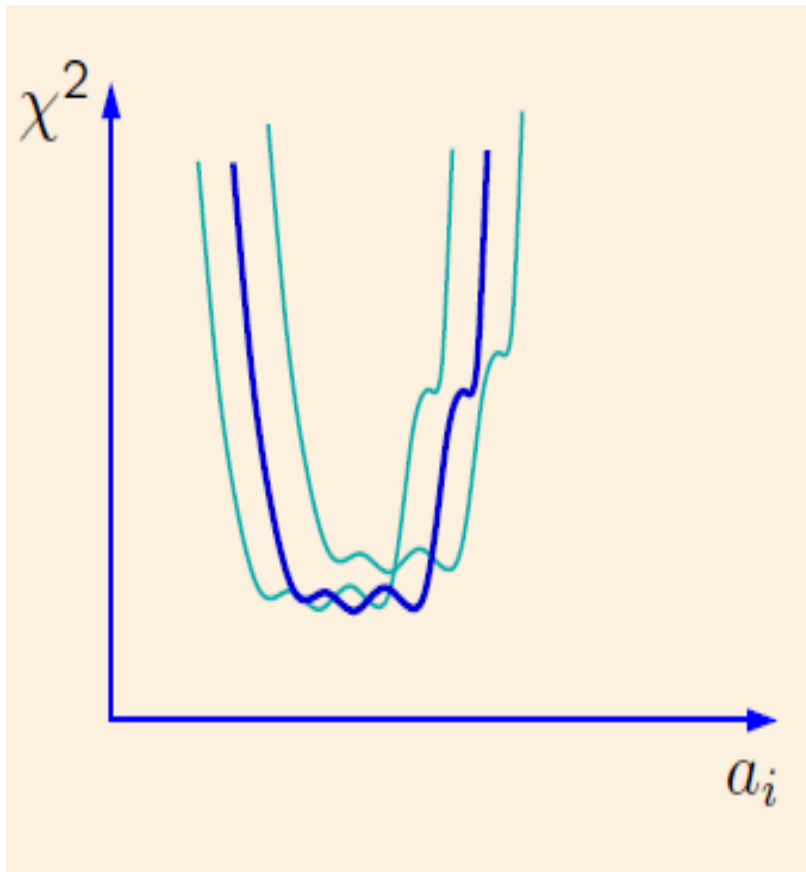
Treating each PDF value  $f_a(x_b, Q_c)$  as a parameter  $a_i$ :



- Establish a confidence region for  $\{a_i\}$  for a given tolerated increase in  $\chi^2$
- In the ideal case of perfectly compatible Gaussian errors, 68% c.l. on a physical observable  $X$  corresponds to  $\Delta\chi^2 = 1$  independently of the number  $N$  of PDF parameters

See, e.g., P. Bevington, K. Robinson, Data analysis and error reduction for the physical sciences

# Error analysis: multiple parametric models, somewhat incompatible experiments

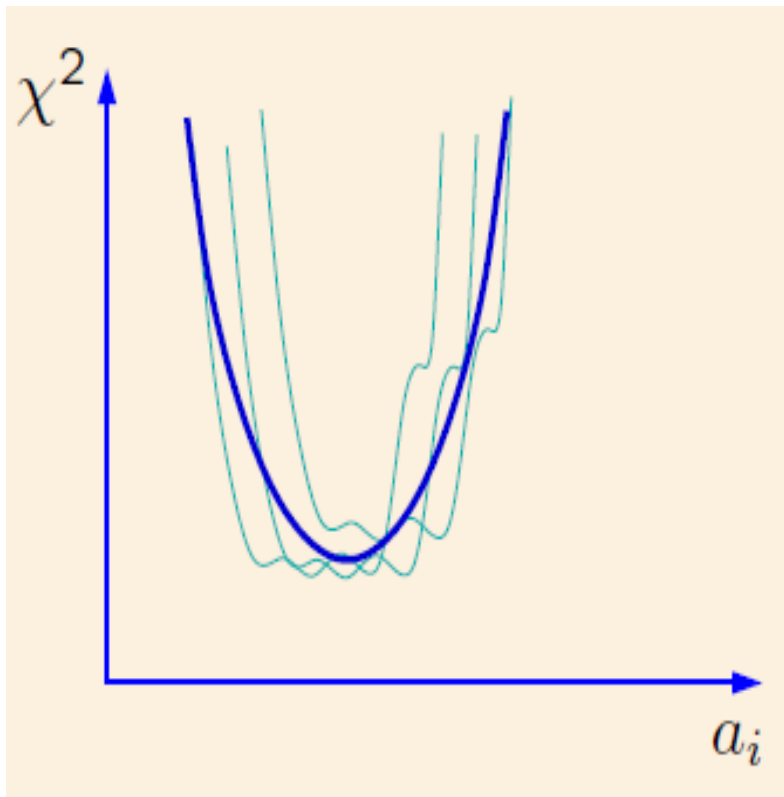


The actual  $\chi^2$  function shows

- a well-pronounced global minimum  $\chi_0^2$
- mild tensions between experiments (a mini-landscape)
- Dependence on the parametrization model and theoretical inputs (which ones?)



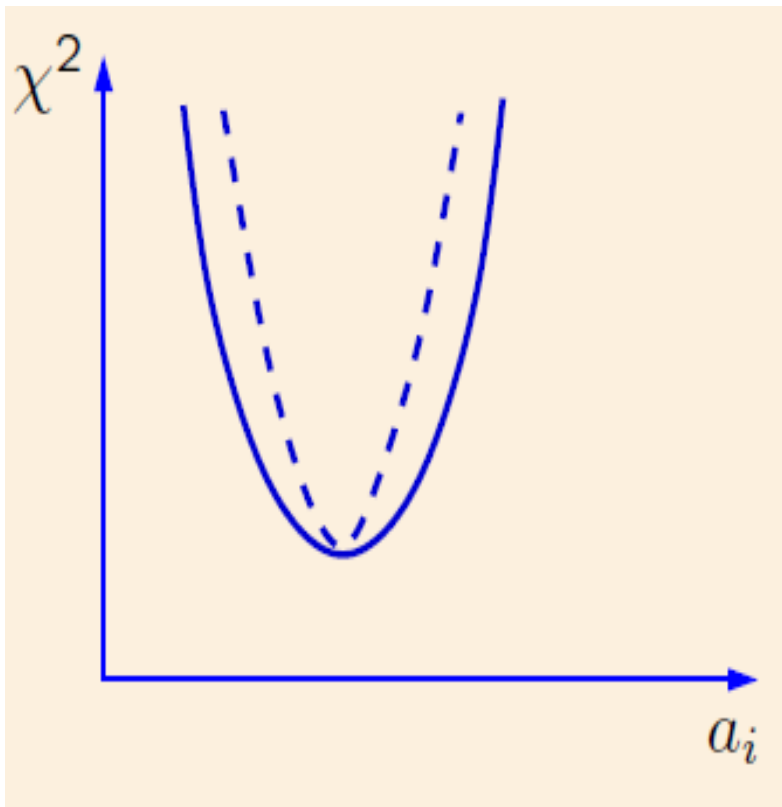
# Error analysis: multiple parametric models, somewhat incompatible experiments



The actual  $\chi^2$  function shows

- a well-pronounced global minimum  $\chi_0^2$
- mild tensions between experiments (a mini-landscape)
- Dependence on the parametrization model and theoretical inputs (which ones?)
- The likelihood is approximately described by a quadratic  $\chi^2$  with a revised tolerance condition  $\Delta\chi^2 \leq T^2$

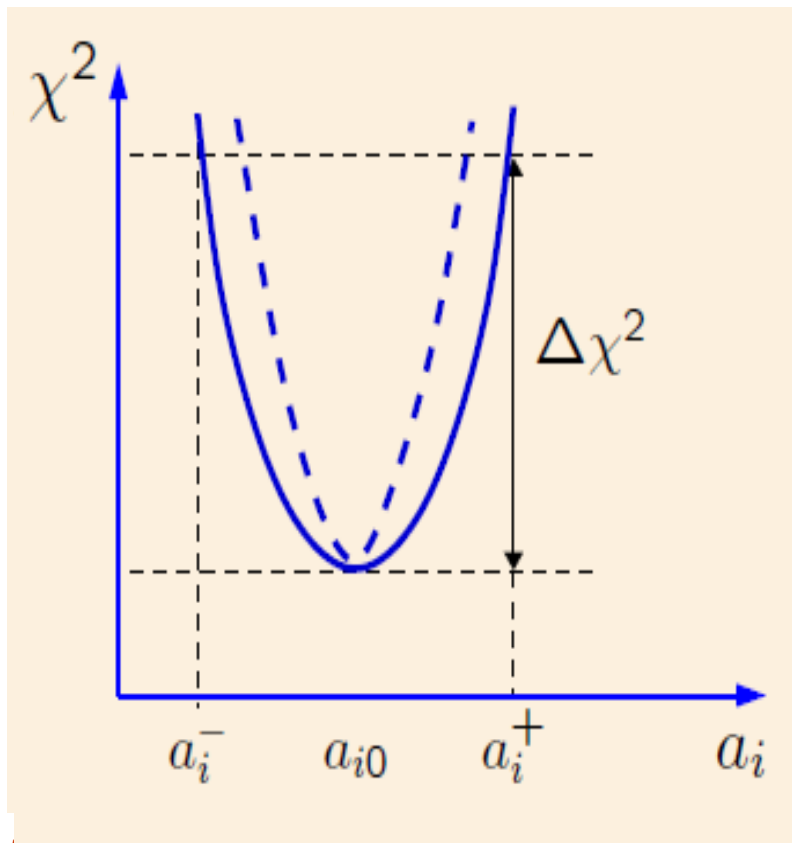
# Error analysis: multiple parametric models, somewhat incompatible experiments



The actual  $\chi^2$  function shows

- a well-pronounced global minimum  $\chi_0^2$
- mild tensions between experiments (a mini-landscape)
- Dependence on the parametrization model and theoretical inputs (which ones?)
- The likelihood is approximately described by a quadratic  $\chi^2$  with a revised tolerance condition  $\Delta\chi^2 \leq T^2$

# Error analysis: multiple parametric models, somewhat incompatible experiments



Tensions between experiments can be accommodated by choosing  $T \sim 2 - 3$  (H. L. Lai et al., 1007.2241; Pumplin, 0909.0268)

Theory uncertainties reduce at NNLO; some residual theory errors can be accounted as systematic nuisance parameters

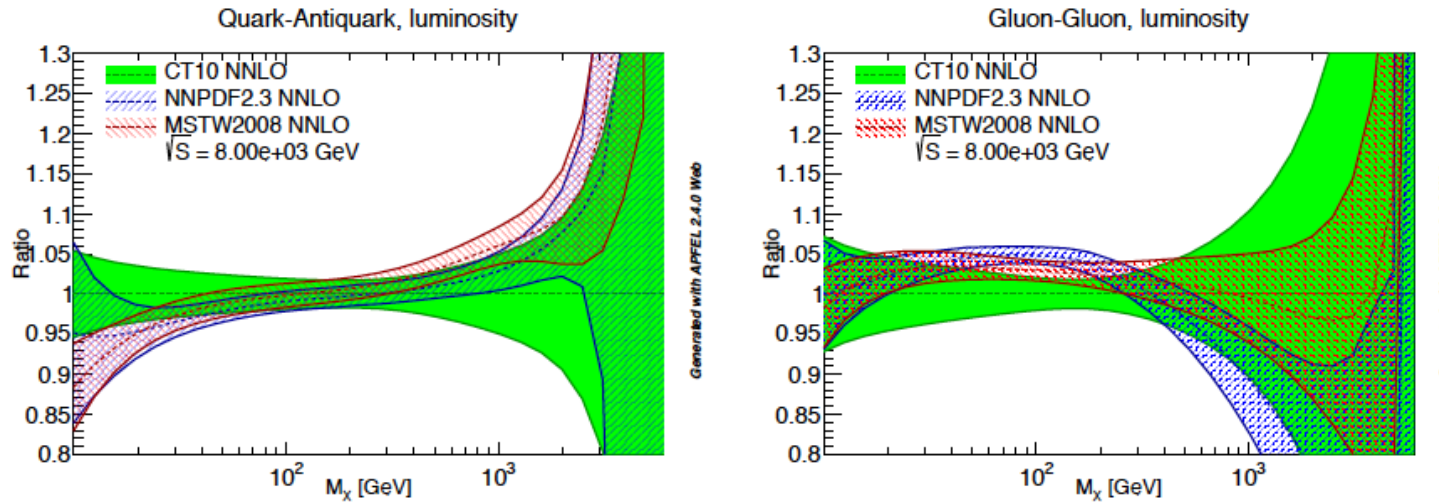
⇒ Progress depends on improved understanding of parametrization uncertainty

⇒ In the context of PDF reweighting, understanding of tolerance will lead to the proper construction of replica weights

# Charm mass dependence of PDFs

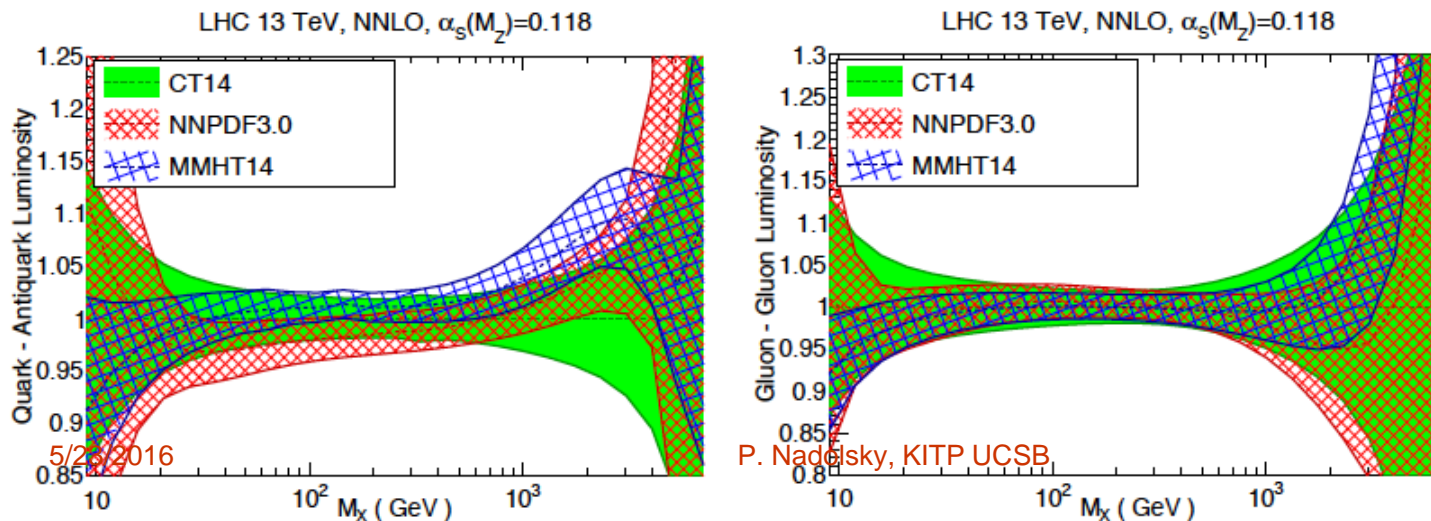
# Reduced META sets

# 2012→2015: Agreement between global NNLO PDFs greatly improved



Note in particular the changes in the gg luminosity, especially important in the Higgs mass region

Figure 1: Comparison of the  $q\bar{q}$  (left) and  $gg$  (right) PDF luminosities at the LHC 8 TeV for CT10, MSTW2008 and NNPDF2.3. Results are shown normalized to the central value of CT10.



LHC data has been added for all 3 new PDFs, but most changes are due to benchmarking of formalisms

5/26/2016

P. Nadolsky, KITP UCSB

# Why global NNLO PDFs are in better agreement now than ever

To start, various NNLO calculations have reduced dependence on renormalization, factorization, and auxiliary mass scales than at NLO

Since 2012, PDF analysis groups carried out a series of benchmarking exercises for key processes of DIS and jet production in PDF fits

Methodologies of all groups were cross-validated and improved.

# Three main uses of PDFs at the LHC

1. Assessment of the total uncertainty on a cross section based on the available knowledge of PDFs, *e.g.*, when computing the cross section for a process that has not been measured yet (such as supersymmetric particle production cross-sections), or for estimating acceptance corrections on a given observable. This is also the case of the measurements that aim to verify overall, but not detailed, consistency with Standard Model expectations, such as when comparing theory with Higgs measurements.
2. Assessment of the accuracy of the PDF sets themselves or of related Standard Model parameters, typically done by comparing theoretical predictions using individual PDF sets to the most precise data available.
3. Input to the Monte Carlo event generators used to generate large MC samples for LHC data analysis.

**For 2), compute cross sections with individual PDF sets.**

For 1) or 3), the PDF uncertainty based on the totality of available PDF sets must be estimated. Estimate the combined PDF error using **an average of various PDF sets.**



# Follow-up publications

## In 2015 Les Houches proceedings

Address questions not covered in the main document of 2015 PDF4LHC recommendation ([arXiv:1510.03865](https://arxiv.org/abs/1510.03865)), and provide illustrations

### 1. Phenomenological applications of PDF4LHC distributions

*J. Gao, T.-J. Hou, J. Huston, P. N., B. Wang, K. Xie, ...*

Physics issues, predictions for typical QCD cross sections

### 2. On the accuracy and Gaussianity of the PDF4LHC15 combined sets of parton distributions

*S. Carrazza, S. Forte, Z. Kassabov, J. Rojo*

Comparisons of PDF4LHC ensembles, non-Gaussian effects

# Choosing the right PDF set for an LHC application

## 6.1 Delivery and guidelines

The PDF4LHC15 combined PDFs are based on an underlying Monte Carlo combination of CT14, MMHT14 and NNPDF3.0, denoted by MC900, which is made publicly available in three different reduced delivery forms:

- PDF4LHC15\_mc: a Monte Carlo PDF set with  $N_{\text{rep}} = 100$  replicas.
- PDF4LHC15\_30: a symmetric Hessian PDF set with  $N_{\text{sig}} = 30$  eigenvectors.
- PDF4LHC15\_100: a symmetric Hessian PDF set with  $N_{\text{sig}} = 100$  eigenvectors.

In the three cases, combined sets are available at NLO and at NNLO, for the central value of  $\alpha_s(m_Z^2) = 0.118$ . In addition, we provide additional sets which contain the central values for  $\alpha_s(m_Z^2) = 0.1166$  and  $\alpha_s(m_Z^2) = 0.1196$ , and that can be used for the computation of the combined PDF+ $\alpha_s$  uncertainties, as explained in Sect. 6.2. Finally, for ease of usage, the combined sets for  $\alpha_s(m_Z^2) = 0.118$  are also presented bundled with the  $\alpha_s$ -varying sets in dedicated grid files. The specifications of each of the combined NNLO PDF4LHC15 sets that are available from LHAPDF6 are summarized in Table 5; note that the corresponding NLO sets are also available.

**Usage of the PDF4LHC15 sets.** As illustrated in Sect. 5, the three delivery options provide a reasonably accurate representation of the original prior combination. However, each of these methods has its own advantages and disadvantages, which make them more suited in different specific contexts. We now attempt to provide some general guidance about which of the three PDF4LHC15 combined sets should be used in specific phenomenological applications.

### 1. Comparisons between data and theory for Standard Model measurements

**Recommendations:** Use individual PDF sets, and, in particular, as many of the modern PDF sets [5–11] as possible.

**Rationale:** Measurements such as jet production, vector-boson single and pair production, or top-quark pair production, have the power to constrain PDFs, and this is best utilized and illustrated by comparing with many individual sets.

As a rule of thumb, any measurement that potentially can be included in PDF fits falls in this category.

The same recommendation applies to the extraction of precision SM parameters, such as the strong coupling  $\alpha_s(m_Z^2)$  [75, 124], the  $W$  mass  $M_W$  [125], and the top quark mass  $m_t$  [126] which are directly correlated to the PDFs used in the extraction.

### 2. Searches for Beyond the Standard Model phenomena

**Recommendations:** Use the PDF4LHC15\_mc sets.

**Rationale:** BSM searches, in particular for new massive particles in the TeV scale, often require the knowledge of PDFs in regions where available experimental constraints are limited, notably close to the hadronic threshold where  $x \rightarrow 1$  [127]. In these extreme kinematical regions the PDF uncertainties are large, the Monte Carlo combination of PDF sets is likely to be non-Gaussian. *c.f.* Figs. 10 and 11.

The PDF4LHC document contains detailed guidelines to help decide which individual or combined PDFs to use depending on the circumstances

To assist in choosing the best PDF(s), demonstrative comparisons were generated of typical LHC cross sections for recent PDFs

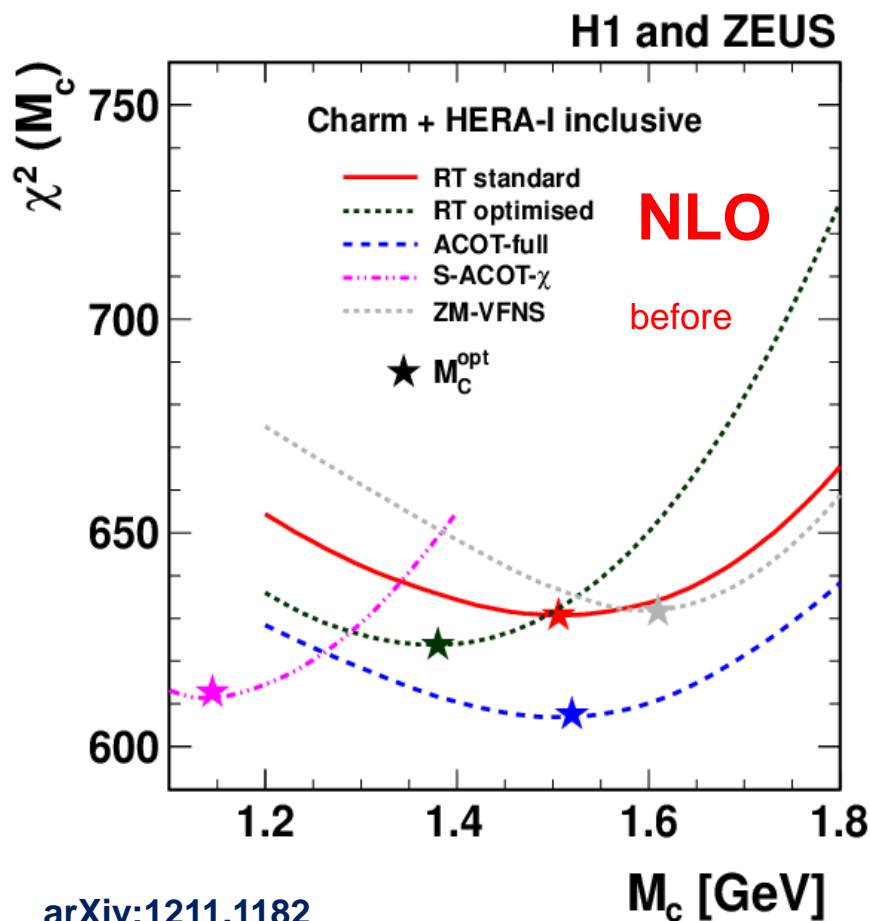
## 1. MC2H gallery of LHC cross sections: ApplGrid, typical experimental cuts

[www.hep.ucl.ac.uk/pdf4lhc/mc2h-gallery/](http://www.hep.ucl.ac.uk/pdf4lhc/mc2h-gallery/)

## 2. META gallery of LHC cross sections: ApplGrid or full calculations, minimal cuts

[Metapdf.hepforge.org/2016\\_pdf4lhc/](http://Metapdf.hepforge.org/2016_pdf4lhc/)

# NLO= $O(\alpha_s)$ : GM-VFN predictions for DIS have large dependence on matching scales

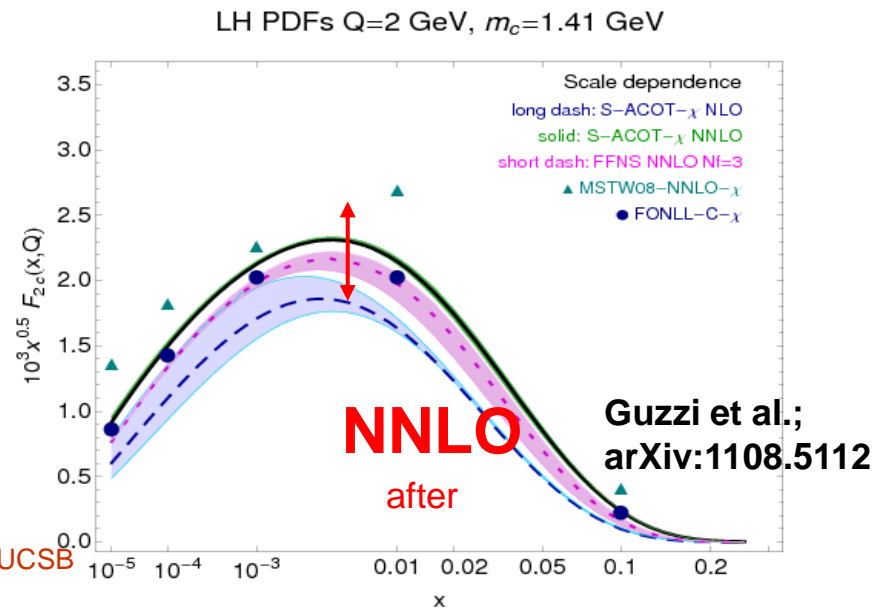
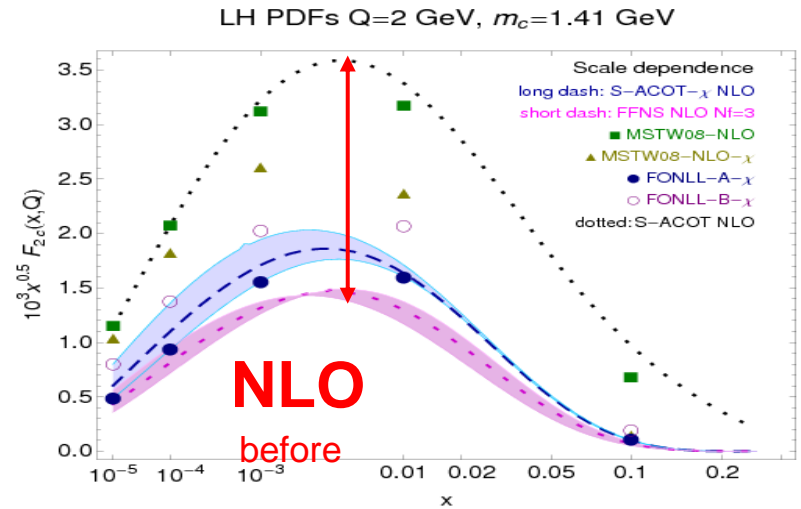
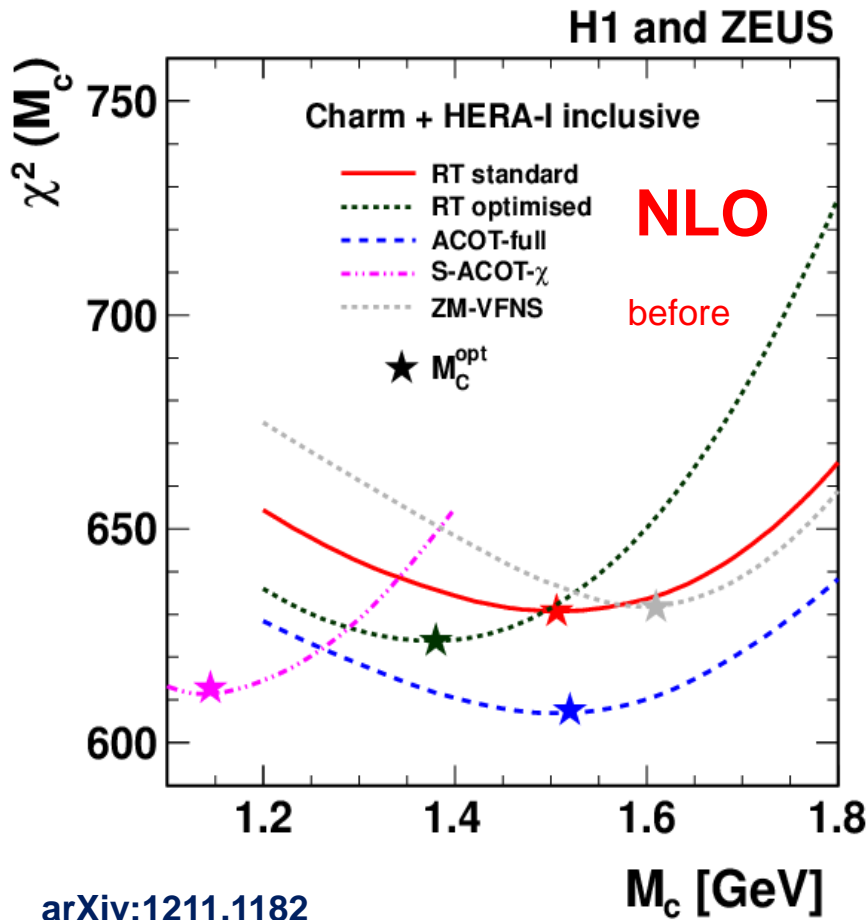


The gluon PDF depends on the factorization scheme used to fit HERA DIS data

Besides the physical mass  $m_c$ , general-mass (GM-VFN) schemes used by global fits introduce matching energy scales of order  $m_c$

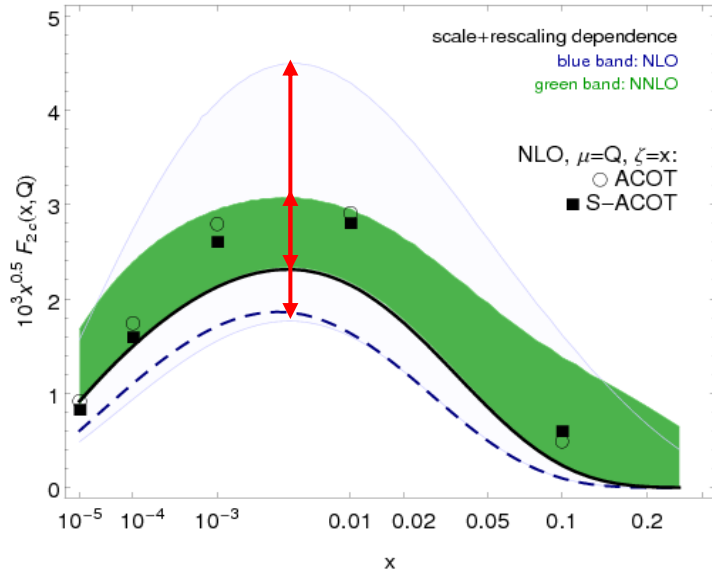
At NLO, uncertainty due to matching parameters is large; each scheme prefers an “optimal”  $m_c$  that brings  $\chi^2$  to comparable levels (cf. the figure)

NNLO= $O(\alpha_s^2)$ : dependence on matching parameters is suppressed,  
GM-VFN schemes are more similar



# GM-VFN schemes are more predictive at NNLO

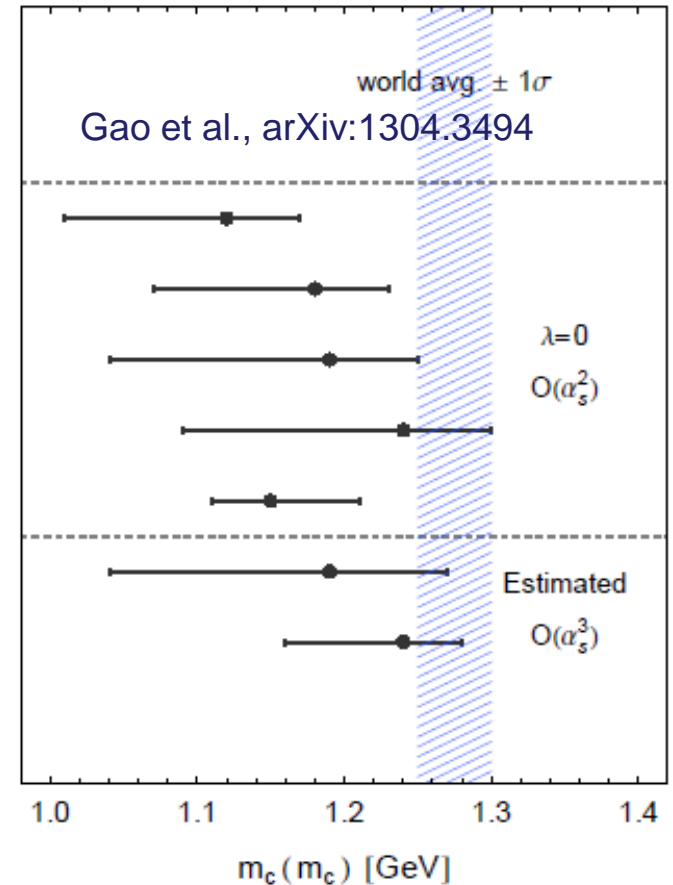
LH PDFs Q=2 GeV S-ACOT



From Guzzi et al.; arXiv:1108.5112;  
see also J. Rojo et al., 1003.1241, p. 110

error at 68% C.L.

1. CT10, fit 1
2. fit 2
3. fit 3
4. fit 4
5. FFN (Alekhin et al.,  $\Delta\chi^2=1$ )
6. CT10, with  $\lambda$  unc.
7. FFN (Alekhin et al.,  $\Delta\chi^2=1$ )



At  $O(\alpha_s^2)$  and approximate  $O(\alpha_s^3)$ , constraints on  $m_c(m_c)$  have been first obtained from combined HERA-I data in the FFN scheme (1212.2355). Constraints on both  $m_c^{pole}$  or  $m_c(m_c)$  in GM-VFNS have been also obtained by CT, MMHT, and NNPDF under varied assumptions. They are comparable with FFNS and the PDG value for  $m_c(m_c)$ .